# OUTPUT ที่ได้จากการวิจัยในโครงการ

# การเผยแพร่ผลงานในวารสารทางวิชาการที่มี peer review

- B. Techaumnat and T. Takuma, Calculation of electric field for lined-up spherical dielectric particles, IEEE Trans. Dielectrics and Electrical Insulation, Vol.10, No.4, pp.623, 2003.
- B. Techaumnat, B. Eua-arporn, and T. Tekuma, Calculation of electric field and dielectrophoretic force on spherical particles in chain, Journal of Applied Physics, Vol.95, No.3, pp.1586, 2004.
- B. Techaumnat and T. Takuma, Electric field and dielectrophoretic force on particles with a surface film, Journal of Applied Physics, Vol.96, No.10, pp.5877, 2004.
- B. Techaumnat, B. Eua-arporn, and T. Takuma, Electric field and dielectrophoretic force on a dielectric particle chain in a parallel-plate electrode system, Journal of Physics D: Applied Physics, Vol.37, pp.3337, 2004.
- B. Techaumnat and T. Takuma, Calculation of electric field and force on conductor particles with a surface film, accepted for publication in IEEE Trans. Magnetics.

# การเผยแพร่ผลงานในการประชุมทางวิชาการระดับนานาชาติ

 B. Techaumnat and T. Takuma, Field intensification at the contact point between a conducting and a spheroid on an elliptic cylinder, to be presented at International Symposium on Electrical Insulation Materials, June 5 – 9, Kitakyushu, Japan.

# ภาคผนวก 🧎

ภาคผนวกนี้แสดง สำเนาของบทความที่ได้รับการตีพิมพ์ในวารสารทางวิชาการจำนวน 5 บทความ และบท ความที่ได้นำเสนอในการประชุมทางวิชาการระดับนานาชาติจำนวน 1 บทความ.

# Calculation of the Electric Field for Lined-up Spherical Dielectric Particles

## Boonchai Techaumnat

Department of Electrical Engineering Faculty of Engineering, Chulalongkorn University Phyathai Road, Pathumwan, Bangkok 10330, Thailand

### and Tadasu Takuma

Central Research Institute of Electric Power Industry 2-11-1 Iwado kita, Komae-shi, Tokyo 201-8511, Japan

### ABSTRACT

This paper calculates the electric field in arrangements of dielectric particles. An analytical method is presented in the paper. The method repetitively inserts monopoles and multipoles until all the boundary conditions are satisfied, so that unlike the existing methods, it does not require setting up a linear equation system in the calculation. It can be applied to various types of energization such as a uniform field, spherical electrodes, or planar electrodes. The method and the BEM, a numerical method, have been utilized to investigate the effects of the particle number and particle permittivity. The authors have compared the results by the analytical method with those by the numerical method, and found that the accuracy of the numerical method greatly varies from less than 10-4% to more than 2%, depending on the condition of the calculation arrangements.

Index Terms — Electrorheological fluid, dielectrophoresis, electric field, analytical method, boundary element method.

# INTRODUCTION

VARIOUS applications of dielectric materials are now advancing in the forms of dielectric particles immersed in a fluid dielectric. For example, electrorheological (ER) fluid [1,2] utilizes the interaction between particles in a fluid dielectric. In these applications, we are usually interested in the amount of force acting on partides which can be often modeled as dielectric spheres. Since the force highly depends on the electric field on the particle surface [3], the precise calculation of the electric field is important for these applications. Generally, the electric field can be calculated either by analytical methods or by mumerical field calculation. The analytical methas give the exact solution of electric field, but are not have applicable for a practical arrangement, especially where a calculation arrangement is complicated. On the contrary, numerical methods can calculate the electric field for theoretically any complicated arrangement, but the accuracy of the results may be sometimes questionthe because of such factors as imperfect shape simulation, improper subdivision, and in some cases singular nature of the electric field in the arrangement.

For an arrangement of two dielectric spheres lying in another dielectric under a uniform electric field, analytical methods for calculating electric field have been presented in bispherical coordinates and in spherical coordinates. Davis [4] and Stoy [5,6] utilized a bispherical coordinate system to express the surface of both dielectric spheres. The potential is expressed by an infinite series, of which the coefficients are recursively determined. A main disadvantage of their approach is that the number of dielectric spheres is limited to only two. On the other hand, Washizu et al. [7] presented a sophisticated method in spherical coordinates. The method utilizes the re-expansion of monopoles and multipoles. It can calculate the field for both axisymmetrical and three-dimensional arrangements. Nakajima et al. [8] extended the method in references [7] to calculate the field for an arrangement consisting of a number of dielectric particles. These two methods express the potential by an infinite series individually for each dielectric sphere. Coefficients in the series are calculated by solving a linear equation system formed by using

Manufactured on 5 December 2002, in final form 26 March 2003.

he boundary conditions on every sphere surface. The dinensions of the linear equation system depend on the number of expansion terms used to represent the infinite enes and the number of dielectric particles. Furthermore, the methods have been proposed only for arrangements energized by an external electric field.

In this paper, we report the calculation of electric field for an arbitrary number of dielectric spheres arranged on line by using analytical and numerical methods. Compured with the methods in references [7] and [8], our ana-

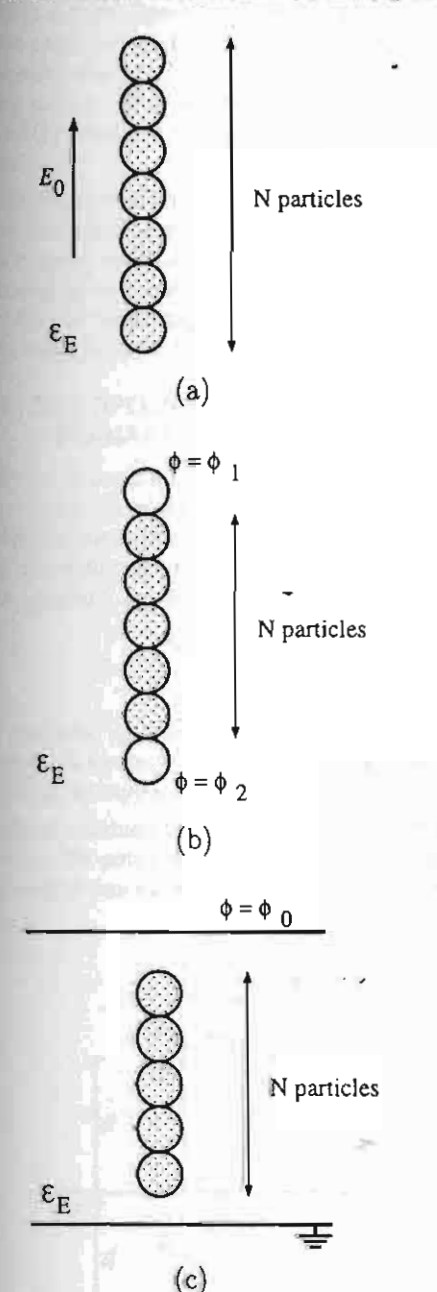


Figure 1. Arrangements of dielectric particles energized by: a, uniform electric field; b, spherical electrodes; c, parallel-plate elec-

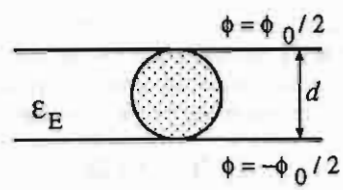


Figure 2. A dielectric particle lying between parallel-plate conductors.

lytical method does not require setting up a linear equation system. Instead, it repetitively inserts multipoles (including monopoles) until all the boundary conditions on conductor and dielectric surfaces are satisfied. Our method requires much less memory capacity compared with the Nakajima et al. calculation. Both the analytical method proposed here and the numerical method can calculate various arrangements consisting of spherical electrodes or planar electrodes. The analytical and numerical methods are further discussed on their advantages and disadvantages.

### ANALYTICAL METHOD

Figures 1a to 1c show examples of arrangements to which the analytical method can be applied. In Figure 1, N dielectric particles are immersed in a fluid dielectric having a permittivity of  $\epsilon_E$ . The radius and permittivity of particles are arbitrary and may be different from each other. A particle may also be in contact with or separated from its adjacent particles. The arrangements are energized by a uniform field as in Figure 1a, by spherical conductors as in Figure 1b, or by parallel-plate conductors as in Figure 1c. When the number of particles is infinitely large in Figure 1a, the arrangement is reduced to a simple one as shown in Figure 2 where a dielectric particle lies between and in contact with two parallel-plate conductors. The arrangement is also equivalent in electric field to the arrangement of Figure 1c where  $N=2^n$  (n=0,1,2,....) dielectric particles are lined in contact with parallel-plate electrodes.

The method utilizes the multipole re-expansion (Appendix 7.1) to express the potential by a set of functions expanded around each particle center. For each particle, we take its center as the origin of spherical coordinates, the potentials  $\phi_I$  in the interior of the particle, and  $\phi_E$  in the exterior of the particle are written as [9]

$$\phi_I = \sum_{j=0}^{\infty} A_j r^j P_j(\cos \theta)$$
 (1)

$$\phi_I = \sum_{j=0}^{\infty} A_j r^j P_j(\cos \theta)$$

$$\phi_E = \sum_{j=0}^{\infty} M_j r^j P_j(\cos \theta) + \sum_{j=0}^{\infty} \frac{B_j}{r^{j+1}} P_j(\cos \theta)$$
(2)

where r and  $\theta$  are the spherical coordinates,  $P_i$  the Legendre function of the first kind, and  $A_j$ ,  $B_j$ ,  $M_j$  are the coefficients of the analytical solutions. The term  $B_i P_i(\cos\theta)/r^{j+1}$  in Equation (2) corresponds to a monopole for j = 0 and a multipole for j > 0.  $B_i$  is denoted as the magnitude of the monopole or multipole. Note that the definition of a multipole is simplified here and slightly different from that in [7]. The first term on the right-hand side of equation (2) is interpreted as the potential due to sources in the exterior of the sphere, while the second term is the potential due to the existence of the sphere. In our method, the coefficients  $A_i$ ,  $B_i$ , and M; are to be recursively adjusted via insertion of monopoles and multipoles so as to satisfy all the boundary conditions in the arrangement. Examples of the application of the analytical method are given in Appendix 7.2 for the arrangements of (1) a point charge and a grounded conducting sphere, (2) a point charge and a dielectric sphere, and (3) a charged conducting sphere and a dielectric sphere.

In the following sections, we first review the potential due to the presence of a multipole and a dielectric particle or a conductor, which is obtained by the proper insertion of monopoles and multipoles. Then, we give a recursive procedure for calculating electric field in the arrangements shown in Figures 1 and 2.

# 2.1 MULTIPOLE AND A GROUNDED PLANAR CONDUCTOR

Consider a k-th order multipole having a magnitude  $B_k$ , located at a point m which lies at a distance d from a grounded planar conductor, as shown in Figure 3. The direction of the multipole is denoted by an arrow in the figure. The potential  $\phi_m$  due to the multipole is

$$\phi_m = \frac{B_k}{r_m^{k+1}} P_k(\cos \theta_m) \tag{3}$$

In this equation,  $r_m$  and  $\theta_m$  are the spherical coordinates where **m** is treated as the origin and  $\theta_m = 0$  in the direction of the multipole.

If the planar conductor is perpendicular to the multipole direction, the potential resulting from the multipole and the conductor can be readily determined by using the

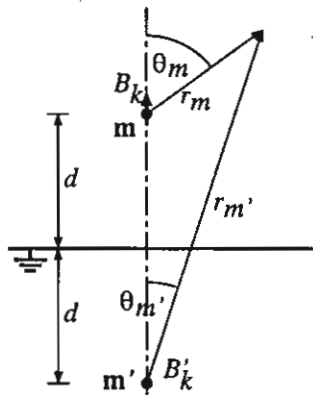


Figure 3. Multipole and a grounded planar conductor.

method of images. In order to satisfy the zero-potential condition on the conductor, an image  $B'_k$  is placed below the conductor by the same distance d (also shown in Figure 3). The magnitude  $B'_k$  of the image is

$$B_k' = (-1)^{k+1} B_k \tag{4}$$

According to the multipole and its image, the potential becomes

$$\phi = \frac{B_k}{r_m^{k+1}} P_k(\cos \theta_m) + (-1)^{k+1} \frac{B_k}{r_{m'}^{k+1}} P_k(\cos \theta_{m'}) \quad (5)$$

where  $r_{m'}$  and  $\theta_{m'}$  are defined in a similar manner to  $r_m$  and  $\theta_m$ . If we re-expand the term  $P_k(\cos\theta_{m'})/r_{m'}^{k+1}$  around m (Appendix 7.1), the potential can be rewritten as

$$\phi = \frac{B_k}{r_m^{k+1}} P_k(\cos \theta_m) + \sum_{j=0}^{\infty} M_j r_m^j P_j(\cos \theta_m)$$
 (6)

for  $r_m < 2d$ .  $M_j$  is the coefficient computed from  $B_k$  by equation (18) in Appendix 7.1.

# 2.2 MULTIPOLE AND A GROUNDED CONDUCTOR SPHERE

Consider a k-th order multipole having a magnitude  $B_k$ , located at a point  $\mathbf{m}$  above a grounded conductor sphere as shown in Figure 4. In the figure,  $\mathbf{n}$  is the center,  $R_n$  is the radius of the sphere, and d is the distance between the multipole and sphere center. The potential  $\phi_m$  due to the multipole is given by equation (3). We re-expand the  $\phi_m$  around  $\mathbf{n}$  (Appendix 7.1) and rewrite  $\phi_m$  as

$$\phi_m = \sum_{j=0}^{\infty} M_{nj} r_n^j P_j(\cos \theta_n), \quad \text{for } r_n < d$$
 (7)

In this equation,  $M_{nj}$  is the coefficient obtained from the re-expansion, where  $r_n$  and  $\theta_n$  are defined in a similar manner to  $r_m$  and  $\theta_m$  in equation (3).

From equation (7), the potential resulting from the multipole and the conductor sphere can be written in a

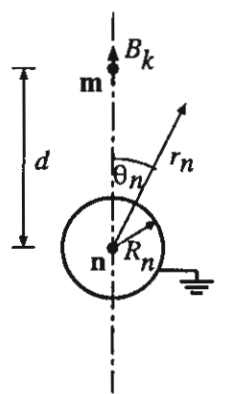


Figure 4. Multipole and a grounded conductor sphere.

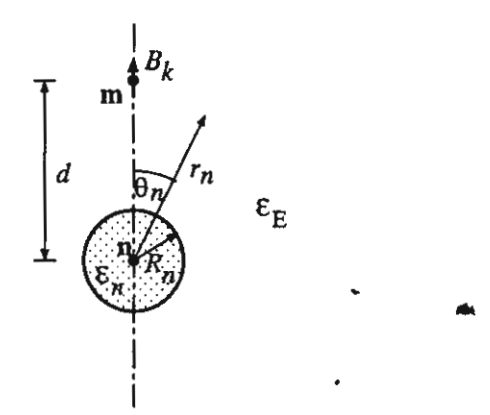


Figure 5. Multipole and a dielectric sphere.

general form of equation (2) around n.

$$\phi = \sum_{j=0}^{\infty} M_{nj} r_n^j P_j(\cos \theta_n) + \sum_{j=0}^{\infty} \frac{B_{nj}}{r_n^{j+1}} P_j(\cos \theta_n)$$
 (8)

By applying the zero-potential condition on the conductor surface, we obtain

$$B_{nj} = -M_{nj}R_n^{2j+1} (9)$$

for j = 0,1,... Thus, the resultant potential becomes

$$\phi = \sum_{j=0}^{\infty} M_{nj} \left[ r_n^j - \frac{R_n^{2j+1}}{r_n^{j+1}} \right] P_j(\cos \theta_n)$$
 (10)

# 2.3 MULTIPOLE AND A DIELECTRIC SPHERE

Consider a multipole and a dielectric sphere in Figure 5. The arrangement is the same as that in Figure 4, except that the conductor sphere is now replaced by a dielectric sphere. The permittivity of the dielectric sphere and the surrounding medium are denoted by  $\epsilon_n$  and  $\epsilon_E$ , respectively.

Similarly as in the previous section, the potential  $\phi_m$  due to the multipole can be re-expanded around n and expressed in the form of equation (7). The potential  $\phi_{nl}$  in the interior of the sphere and  $\phi_{nE}$  in the exterior of the sphere can be written in the forms of equations (1) and (2).

$$\phi_{nI} = \sum_{j=0}^{\infty} A_{nj} r_n^j P_j(\cos \theta_n)$$
 (11)

$$\phi_{nE} = \sum_{j=0}^{\infty} M_{nj} r_n^j P_j(\cos \theta_n) + \sum_{j=0}^{\infty} \frac{B_{nj}}{r_n^{j+1}} P_j(\cos \theta_n) \quad (12)$$

where  $M_{nj}$  is the coefficient in equation (7) obtained by the re-expansion,  $A_{nj}$  and  $B_{nj}$  are the coefficients to be determined so as to satisfy the boundary conditions on the sphere surface. The boundary conditions on the surface

are, at 
$$r_n = R_n$$

$$\phi_{nI} = \phi_{nE}$$

and

$$\epsilon_n \frac{\partial \phi_{nI}}{\partial r_n} = \epsilon_E \frac{\partial \phi_{nE}}{\partial r_n}$$

From the boundary conditions,  $A_{nj}$  and  $B_{nj}$  in equations (11) and (12) are related to  $M_{nj}$  as

$$A_{nj} = \frac{\epsilon_E(2j+1)}{(\epsilon_n + \epsilon_E)j + \epsilon_E} M_{nj}$$
 (13)

$$B_{nj} = (R_n)^{2j+1} \frac{(\epsilon_E - \epsilon_n)j}{(\epsilon_n + \epsilon_E)j + \epsilon_E} M_{nj}$$
 (14)

for j = 0,1,...

### 2.4 PROCEDURE TO CALCULATE THE ELECTRIC FIELD

Consider the arrangements of N particles in Figure 1. Each spherical conductor or dielectric is denoted by a number n = 1, 2, ..., N for convenience. The potential in the interior of the n-th particle is expressed by

$$\phi_{nl} = \sum_{j=0}^{\infty} A_{nj} r_n^j P_j(\cos \theta_n)$$

The potential in the exterior of the n-th particle, is expressed by

$$\phi_{nE} = \sum_{j=0}^{\infty} \left[ M_{nj} r_n^j + \frac{B_{nj}}{r_n^{j+1}} \right] P_j(\cos \theta_n)$$

In the following procedure, we recursively calculate the coefficients  $A_{nj}$ ,  $B_{nj}$  and  $M_{nj}$ . For example, in the *l*-th step of the recursion, we compute  $A_{nj}^{(l)}$ ,  $B_{nj}^{(l)}$  and  $M_{nj}^{(l)}$  and adjust the coefficients as

$$A_{nj} + A_{nj}^{(l)} \Rightarrow A_{nj}$$

$$B_{nj} + B_{nj}^{(l)} \Rightarrow B_{nj}$$

$$M_{ni} + M_{ni}^{(l)} \Rightarrow M_{ni}$$

The recursive procedure is carried out as follows.

1. If an *n*-th conductor sphere possesses a potential  $\phi_n$ , insert a monopole of a magnitude  $B_{n0}^{(0)} = \phi_n R_n$  at the sphere center **n**. So the potential  $(\phi_n)_m$  due to this monopole is

$$(\phi_n)_m = \frac{B_{n0}^{(0)}}{r_n} P_0(\cos \theta_n)$$

Then, separately satisfy the potential boundary condition on each conductor. If there is an external field or a field given by parallel-plate conductors, apply an appropriate value of a constant field  $E_0$ . The potential is then

$$(\phi_n)_m = \pm E_0 r_0 P_1(\cos \theta_0)$$

where  $r_0$  and  $\theta_0$  are the spherical coordinates with the origin being the point of zero potential on the axis of symmetry. The  $\pm$  sign indicates the direction of the external field or the potential difference between the conductors.

2. For each dielectric sphere, re-expand all the monopoles and the external field in step 1 around the particle center n, and add the results to  $M_{nj}^{(0)}$ . For a monopole, utilize equation (18) or (19) in Appendix 7.1 to compute  $M_{nj}^{(0)}$  (j = 0,1,...). For the case of an external field

$$M_{n0}^{(0)} = \phi_{n0}$$
 $M_{n1}^{(0)} = \pm E_0$ 

where  $\phi_{n0}$  is the potential due to  $E_0$  at n, and  $M_{nj}^{(0)} = 0$  for  $j \neq 0,1$ .

- 3. Compute the coefficients  $A_{nj}^{(0)}$  and  $B_{nj}^{(0)}$  (j=0,1,...) of each dielectric sphere from  $M_{nj}^{(0)}$  by using equations (13) and (14). After this step, we compute  $A_{nj}^{(0)}$ ,  $B_{nj}^{(0)}$ , and  $M_{nj}^{(0)}$  for n=1,2,...,N and j=0,1,... (For an n-th conductor sphere, all  $A_{nj}$  are zero.)
- 4. For each conductor sphere and dielectric one, re-expand the multipoles  $B_{mk}^{(0)} P_k(\cos \theta_m) / r_m^{k+1}$  (k=0,1,...) of all the other conductors and spheres (for all  $m \neq n$ ) around its center, and accumulate the results to  $M_{ni}^{(1)}$ .
  - 5. Compute  $A_{nj}^{(1)}$  and  $B_{nj}^{(1)}$
- For a planar electrode, simply calculate  $B_{nj}^{(1)}$  by using equation (4).
- For a conductor sphere, compute  $B_{nj}^{(1)}$  by using equation (9).
- For a dielectric sphere, compute  $A_{nj}^{(1)}$  and  $B_{nj}^{(1)}$  by using equations (13) and (14).
- 6. Repeat steps 4 and 5, re-expand  $B_{mk}^{(l)}$  to  $M_{nj}^{(l+1)}$  and calculate  $B_{nj}^{(l+1)}$  from  $M_{nj}^{(l+1)}$ , until the solution converges.

### 3 NUMERICAL METHOD

Numerical field calculation methods have already been applied as a practical way to obtain the field distribution on the dielectric particles [10–12]. Numerical field calculation methods can be classified into two categories; domain subdivision methods and boundary subdivision methods. In this paper, we have utilized the boundary element method (BEM) which is one of the boundary subdivision methods. In the BEM, the electric scalar potential and the normal component of electric field in the outward direction on all the boundary nodes are determined first. Then, the potential  $\phi_p$  at any point p in the region can be expressed in terms of the potential  $\phi$  and the normal component of electric field  $E_n$  on the boundary  $\Gamma$  of the region as

$$C\phi_{p} = \int_{\Gamma} E_{n} \phi^{*} d\Gamma + \int_{\Gamma} \phi (\partial \phi^{*} / \partial n) d\Gamma$$
 (15)

where C is a coefficient that depends on the position of p,  $\phi^*$  the fundamental solution of the Poisson equation  $\nabla^2 \phi^* = -\Delta^p (\Delta^p)$  is a Dirac delta function that is every-

where 0 except at p.), and  $(\partial \phi^*/\partial n)$  is its normal derivative on the boundary. C = 1 if p is not on the boundary. If p is on the boundary and the boundary is smooth at p, C = 1/2. The BEM can be applied to an inhomogeneous domain by subdividing the domain into regions of each homogeneous medium. The values between two adjacent regions, region 1 and 2, are related on the boundary interface as

$$\phi_1 = \phi_2$$

$$\epsilon_1 E_{n1} = \epsilon_2 E_{n2}$$

where  $\epsilon$  is the permittivity of each region and the subscripts 1 and 2 denote the region.

As the electric field can become very high in complex dielectric cases, substantially increasing with particle permittivity, numerical field calculations must be appropriately implemented in order to minimize calculation er-

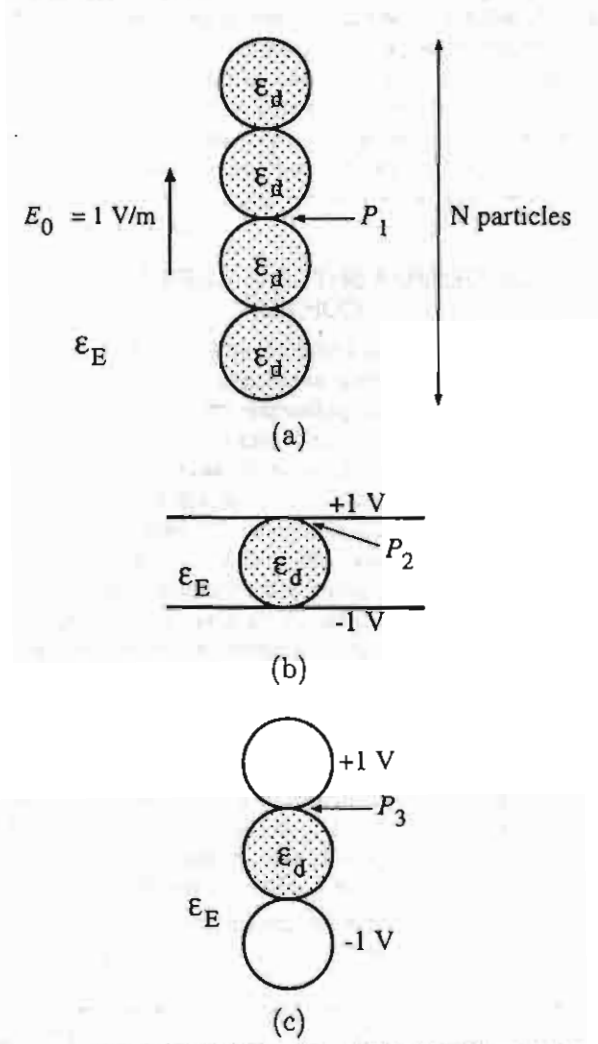


Figure 6. Calculation arrangements. a, N dielectric spheres under a uniform field; b, one dielectric sphere under parallel-plate conductors; c, one dielectric sphere between two spherical conductors.

rors. We have simulated every surface contour with second-order curved elements, and utilized second-order polynomial interpolating functions for the potential and electric field on the elements. Each sphere contour has been subdivided into 360 elements between  $\theta = 0$  to  $\pi$ .

### 4 CALCULATION RESULTS

Figure 6 shows arrangements of which we have calculated the electric field by the two methods. The arrangements in Figures 6a and 6b consist of N and an infinite number of dielectric spheres under a uniform electric field of 1 V/m, respectively. As already explained, the electric field of Figure 6b is also the same as that in Figure 1c where  $N = 2^n$  spheres are in contact with parallel-plate electrodes. The arrangement in Figure 6c is a dielectric sphere subjected to a non-uniform electric field between two conductor spheres. In this case, the average electric field is kept to be 1 V/m, as same as in the other arrangements. All dielectric spheres in each arrangement have the same permittivity  $\epsilon_d$  which has been varied from 1 to 64 times of the exterior permittivity  $\epsilon_E$  in the calculation. Radii of all the dielectric and conductor spheres are set to a unit length of 1 m.

# 4.1 RESULTS BY THE ANALYTICAL METHOD

Calculation results for all the arrangements are presented in Figure 7. Figure 7 shows the electric field at contact points between the dielectric particles or between a dielectric particle and a conductor. The contact points are the points  $P_1$  to  $P_3$  denoted in Figure 6. We display the contact-point electric field here because the field is usually maximum at a contact point, providing the dielectric spheres are perfectly insulating, i.e. they possess no conductivity [10]. It is clearly seen from the figure that for the energization by a uniform field, the contact-point electric field increases with increasing the number of dielectric spheres from two  $(P_1, N = 2)$  to four  $(P_1, N = 4)$ , eight  $(P_1, N = 8)$ , and infinity  $(P_2)$ . However, an infinite

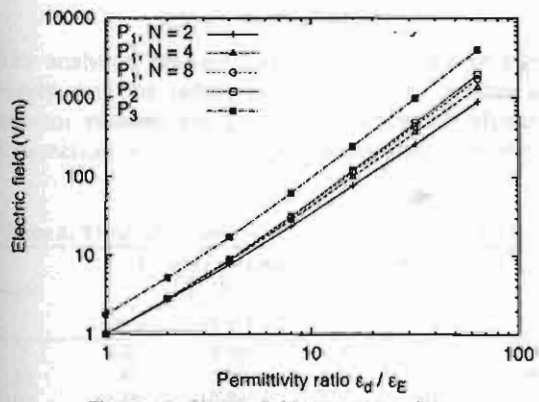


Figure 7. Electric field at contact points.

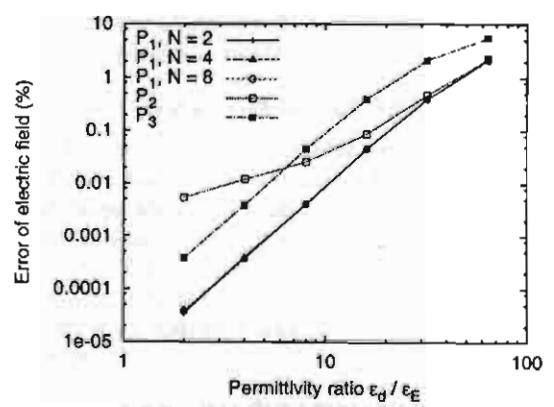


Figure 8. Errors of the electric field by BEM.

number of spheres does not lead to a singular field on particle surface. The field is even lower than that in the case of spherical conductors  $(P_3)$ . Concerning the effect of particle permittivity, the contact-point electric field is greatly intensified by an increase of  $\epsilon_d/\epsilon_E$  as can be seen in Figure 7 presented in logarithmic scale. The slope of each line in the relation between the electric field and the permittivity ratio gradually increases with the permittivity ratio. For example, the slope for  $P_3$  increases approximately from 1.83 at  $\epsilon_d/\epsilon_E = 6$  to 1.93 at  $\epsilon_d/\epsilon_E = 12$ , and 1.98 at  $\epsilon_d/\epsilon_E = 48$ .

# 4.2 RESULTS BY THE NUMERICAL METHOD

Calculation results by the BEM are presented in Figure 8, which shows the errors of the contact-point electric field compared with the corresponding analytical results in the previous section. It is clear that the results by the BEM agree well with those of the analytical method. However, the accuracy of the numerical method (BEM) decreases when the permittivity of dielectric spheres becomes higher. The field non-uniformity in the case of spherical conductors  $(P_3)$  also magnifies the errors in calculation results. In Figure 8, the error at  $P_2$  exhibits a different pattern from the others. The error is comparatively higher at low  $\epsilon_d/\epsilon_E$ . The higher error is caused by the difficulty in numerical calculation. Figure 9 depicts the simulated surface of the dielectric sphere and planar conductor near the contact point P2. A distance between adjacent points in the figure represents an element size. It is clearly seen from the figure that the two surfaces are extremely close to each another near P2, thus making the numerical calculation very difficult to realize a high accuracy.

For all the arrangements, the errors shown in Figure 7 rise from less than  $10^{-2}$  or  $10^{-4}\%$  to more than 2% when

P<sub>2</sub>

sphere surface  $\circ$ conductor surface  $\circ$ Figure 9. Subdivision near the point  $P_2$ .

Table 1. Values of k for all the calculated arrangements.

Contact Point	$P_1$			$P_2$	P <sub>3</sub>
	N = 2	N = 4	N = 8		
k	0.7859	0.8893	0.9460	0.9713	1.0123

the particle permittivity increases from 2 to 64. It is to be noted here that the error can be much higher for a coarser subdivision of sphere surface or the use of linear elements instead of curved elements.

# 5 DISCUSSIONS 5.1 APPROXIMATION OF CONTACT-POINT ELECTRIC FIELD

The following approximation expression has been proposed for the electric field  $E_c$  at a contact point in the  $\epsilon_E$  side [13].

$$\frac{E_c}{E_{c1}} = \frac{1}{2} \left( \epsilon_d / \epsilon_E \right) \left( \left( \epsilon_d / \epsilon_E \right)^k + 1 \right) \tag{16}$$

where  $E_{c1}$  is the contact-point electric field for  $\epsilon_d/\epsilon_E=1$ , and k is a constant depending on arrangement conditions. Table 1 shows the estimated values of k for all the calculated arrangements. They are determined from the analytical results in the range of  $\epsilon_d/\epsilon_E=1$  to 64. For the case of a uniform external field  $(P_1 \text{ and } P_2)$ , all the values of k in Table 1 are smaller than 1.0 as predicted in [13]. However, the table shows that k is possibly greater than 1.0 if a dielectric sphere is subjected to a non-uniform field  $(P_3)$ . Table 2 shows the errors evaluated from the analytical results when the values of k in Table 1 are used to estimate the electric field.

# 5.2 COMPARISON OF THE ANALYTICAL AND NUMERICAL METHODS

For the calculation of the electric field on dielectric spheres in another dielectric medium, we have shown the results by the analytical method and the numerical field calculation method. The methods may be compared in the following aspects.

### 5.2.1 ACCURACY

The analytical method gives the field value of higher accuracy than the numerical method since particle and conductor surfaces are perfectly represented. However, the numerical methods can give adequately accurate re-

Table 2. Errors of the electric field obtained by equation (15).

	Errors of the contact-point electric field (%)						
$\epsilon_d/\epsilon_E$	$P_1$			$P_2$	P <sub>3</sub>		
	N = 2	N = 4	N = 8				
4	3.66	4.10	6.28	7.75	4.08		
16	1.41	1.32	2.79	4.08	1.79		
64	1.54	0.69	2.27	4.17	1.44		

sults if they are appropriately implemented as we have shown in the previous section.

#### 5.2.2 APPLICABILITY

The numerical methods are useful for the arrangements where a dielectric or conductor surface is in a more complicated shape where no analytical method is applicable. The analytical method can give correct results without any problem even for some arrangements where the singularity of electric field is concerned, such as an arrangement of two or more spherical dielectrics in contact under a uniform field.

#### 5.2.3 CALCULATION TIME

For the BEM and many other numerical field calculation methods, calculation time increases by  $O(N_e^2)$  where N<sub>e</sub> is the number of elements utilized. N<sub>e</sub> is also explicitly proportional to the particle number  $N_p$ . For the analytical method proposed here, the calculation time also increases by  $O(N_p^2)$  since the number of operations in each iteration is simply proportional to the square of  $N_p$  at a large  $N_p$ . However, the main difference is that while the permittivity ratio  $\epsilon_d/\epsilon_E$  has no effect on the calculation time by the numerical methods, it considerably affects the calculation time by the analytical method. This is because the recursive procedure takes more steps until the results converge for a higher  $\epsilon_d/\epsilon_E$ . So we prefer the use of numerical field calculation methods for the case that the  $\epsilon_d/\epsilon_E$  and particle number are large, provided that the accuracy of the methods is primarily confirmed by the analytical method for the case of a small number of particles. This is based on Figure 8 where the accuracy is virtually independent of a particle number at high  $\epsilon_d/\epsilon_E$ .

Lastly, it is to be noted that although we have proposed and applied the analytical method for axisymmetrical arrangements in this paper, the method can be applied in a similar manner to a three-dimensional arrangement by using the associated Legendre functions.

### 5 CONCLUSIONS

THIS paper has applied an analytical method and a numerical method to calculate electric field on dielectric particles immersed in another dielectric medium. An analytical method has been proposed in this paper. The method can calculate the electric field in axisymmetrical arrangements for a variety of conditions. We have utilized the method and the BEM, a numerical method, to calculate electric field in some representative arrangements and compared the results by the methods. We have found that the maximum electric field increases with the particle number, the particle permittivity, and the degree of non-uniformity of an applied field. The results by the BEM agree well with the analytical results. However, the results by the BEM become less accurate with increasing the permittivity of dielectric particles. We suggest the use

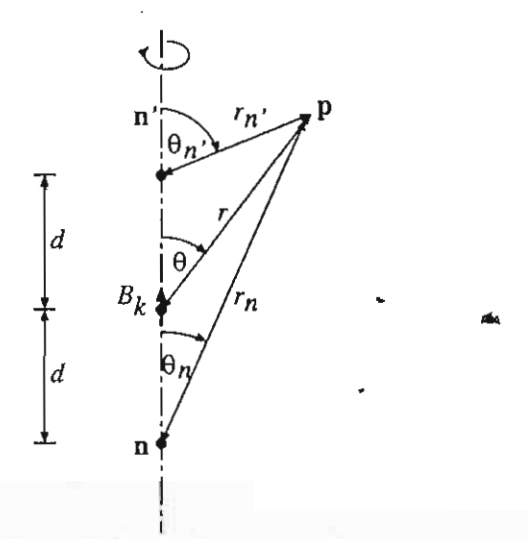


Figure 10. Re-expansion of a multipole.

of the analytical method to estimate the accuracy of the numerical method. The maximum electric field on particle surface can be approximated by using an empirical equation with the proper parameter.

### **ACKNOWLEDGMENT**

This work was supported by the Thailand Research Fund. The authors would like to thank Dr. Shoji Hamada at Kyoto University for his discussions and pieces of ad-

### 7 APPENDICES

#### 7.1 RE-EXPANSION OF A MULTIPOLE

Consider a k-th order multipole of a unit magnitude  $(B_k = 1)$  at the origin of a spherical coordinate system in Figure 10. The potential due to the multipole can be reexpanded around the point  $\mathbf{n}$  or  $\mathbf{n}'$  in the same figure.  $\mathbf{n}$  and  $\mathbf{n}'$  are separated from the multipole by a distance d, and are in the  $\theta = \pi$  and  $\theta = 0$  direction from the multipole, respectively. The re-expansion equations for the potential  $\phi$  at a point  $\mathbf{p}(r,\theta)$  in Figure 10 according to the multipole are

$$\phi = \frac{1}{r^{k+1}} P_k(\cos \theta) \tag{17}$$

$$= \left(\frac{1}{d}\right)^{k+1} \sum_{j=0}^{\infty} \frac{(k+j)!}{k!j!} \left(\frac{-r_{n'}}{d}\right)^{j} P_{j}(\cos\theta_{n'})$$
 (18)

$$= (-1)^{k} \left(\frac{1}{d}\right)^{k+1} \sum_{j=0}^{\infty} \frac{(k+j)!}{k!j!} \left(\frac{r_{n}}{d}\right)^{j} P_{j}(\cos\theta_{n}) \quad (19)$$

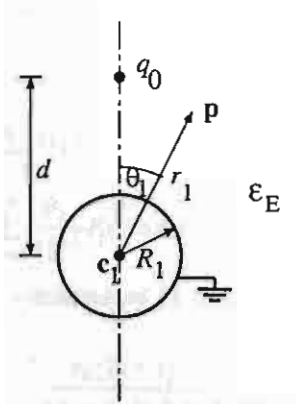


Figure 11. A point charge and a grounded conducting sphere.

These expressions were derived in reference [7].

#### 7.2 CALCULATION EXAMPLES

### 7.2.1 A POINT CHARGE AND A GROUNDED CONDUCTING SPHERE

Consider a point charge  $q_0$  and a grounded conducting sphere of radius  $R_1$  shown in Figure 11. The sphere center is located at  $c_1$  which is separated from  $q_0$  by a distance d. The permittivity of the exterior region is  $\epsilon_E$ . We determine the potential for this arrangement in the following steps.

1. Re-expand the potential  $\phi_{q0}$  due to  $q_0$  at a point p (that  $R_1 < r_1 < d$ ) around the sphere center  $c_1$  by using equation (19) with k = 0 as

$$\phi_{q0} = \frac{q_0}{4\pi\epsilon_E d} \sum_{j=0}^{\infty} \left(\frac{r_1}{d}\right)^j P_j(\cos\theta_1)$$
$$= \sum_{j=0}^{\infty} M_{1j} r_1^j P_j(\cos\theta_1)$$

where  $r_1$  and  $\theta_1$  are the distance and angle shown in Figure 11 and  $M_{1j} = q_0/(4\pi\epsilon_E d^{j+1})$ .

2. Use equation (8) to express the potential  $\phi$  at p as

$$\phi = \sum_{j=0}^{\infty} M_{1j} r \{ P_j(\cos \theta_1) + \sum_{j=0}^{\infty} \frac{B_{1j}}{r_1^{j+1}} P_j(\cos \theta_1)$$

oг

$$\phi = \phi_{q0} + \sum_{j=0}^{\infty} \frac{B_{1j}}{r_1^{j+1}} P_j(\cos \theta_1)$$
 (20)

where  $B_1$ , is determined by using equation (9)

$$B_{1j} = -\frac{q_0}{4\pi\epsilon_E} \frac{R_1^{2j+1}}{d^{j+1}}$$

It can be easily proved that the second term on the right hand side of equation (20) is identical to the potential due to a point charge  $q_1 = -(R_1/d)q_0$  located at a distance of  $R_1^2/d$  from  $c_1$  as shown in Figure 12. Consequently, for

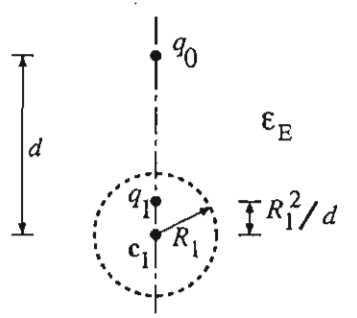


Figure 12. Image charge inside the conducting sphere.

this arrangement the solution obtained by utilizing the multipole re-expansion is simply the same as that obtained by the method of images which can be found in text books on electromagnetics such as [14].

# 7.2.2 A POINT CHARGE AND A DIELECTRIC SPHERE

Consider a point charge  $q_0$  and a dielectric sphere of radius  $R_1$  shown in Figure 13. The dielectric-sphere center is located at  $c_1$  which is separated from  $q_0$  by a distance d. The permittivity of the sphere and the exterior region are  $\epsilon_1$  and  $\epsilon_E$ , respectively. We determine the potential for this arrangement in the following steps.

1. Re-expand the potential  $\phi_{q0}$  due to  $q_0$  at a point p (that  $r_1 < d$ ) around the sphere center  $c_1$  as

$$\phi_{q0} = \sum_{j=0}^{\infty} M_{1j} r \{ P_j (\cos \theta_1) \}$$

where  $r_1$  and  $\theta_1$  are the distance and angle shown in Figure 13 and

$$M_{1j} = \frac{q_0}{4\pi\epsilon_E d^{j+1}}$$

2. Use equations (11) and (12) to express the potential  $\phi$  at p in the following forms.

If p is in the interior of the dielectric sphere

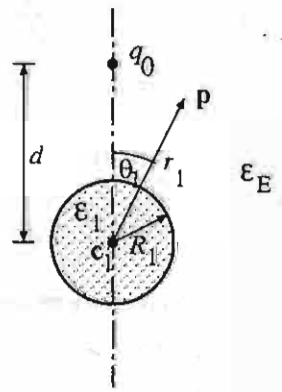


Figure 13. A point charge and a dielectric sphere.

$$\phi = \phi_{1I} = A_{1i} r \{ P_i(\cos \theta_1)$$
 (21)

If p is in the exterior of the dielectric sphere

$$\phi = \phi_{1E} = \sum_{j=0}^{\infty} M_{1j} r \{ P_j(\cos \theta_1) + \sum_{j=0}^{\infty} \frac{B_{1j}}{r_1^{j+1}} P_j(\cos \theta_1)$$

$$= \phi_{q0} + \sum_{j=0}^{\infty} \frac{B_{1j}}{r_1^{j+1}} P_j(\cos \theta_1)$$
(22)

 $A_{1j}$  and  $B_{1j}$  are determined by using equations (13) and (14)

$$A_{1j} = \left\{ \frac{\epsilon_E(2j+1)}{(\epsilon_1 + \epsilon_E)j + \epsilon_E} \right\} \frac{q_0}{4\pi\epsilon_E d^{j+1}}$$
 (23)

$$B_{1j} = (R_1)^{2j+1} \left\{ \frac{(\epsilon_E - \epsilon_1)j}{(\epsilon_1 + \epsilon_E)j + \epsilon_E} \right\} \frac{q_0}{4\pi\epsilon_E d^{j+1}} \quad (24)$$

Note that for the arrangement of a point charge and a dielectric sphere, the solution by the method of images using only point charges is not available since neither the term on the right hand side of equation (21) nor the second term on the right hand side of equation (22) is a potential of a single point charge. The solution for this arrangement can only be obtained by the application of multipoles to express the electric potential  $\phi$ .

# 7.2.3 A CHARGED CONDUCTING SPHERE AND A DIELECTRIC SPHERE

Consider a conducting sphere of radius  $R_1$  and a dielectric sphere of radius  $R_2$  shown in Figure 14. The centers of the conducting and dielectric spheres are located at  $c_1$  and  $c_2$  (separated by a distance d), respectively. The conducting sphere is assumed to have an arbitrary potential  $\phi_1$ . The permittivity of the dielectric sphere and the exterior region are  $\epsilon_2$  and  $\epsilon_E$ , respectively. We determine the potential for this arrangement in the following steps.

L Place a point charge  $q_1 = 4\pi\epsilon_E\phi_1R_1$  (a monopole of a magnitude  $B_{10}^{(0)} = \phi_1R_1$ ) at  $c_1$  to satisfy the boundary condition of the conducting sphere.

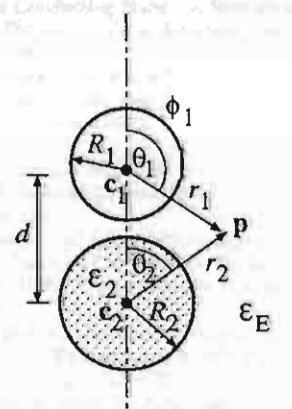


Figure 14. A charged conducting sphere and a dielectric sphere.

2. Re-expand the potential  $\phi_1^{(0)}$  due to  $q_1$  at a point **p** (that  $r_1 > R_1$  and  $r_2 < d$ ) around  $c_2$  as

$$\phi_1^{(0)} = \sum_{j=0}^{\infty} M_{2j} r_2^j P_j(\cos \theta_2)$$

where  $r_1$ ,  $r_2$ , and  $\theta_2$  are the distances and angles shown in Figure 14, and

$$M_{2j}^{(0)} = \frac{q_1}{4\pi\epsilon_E d^{j+1}} = \frac{B_{10}^{(0)}}{d^{j+1}}$$

3. Utilize equations (11) and (12) to express the potential  $\phi$  at p in the following forms.

If p is in the interior of the dielectric sphere

$$\phi = \phi_{2j}^{(0)} = \sum_{j=0}^{\infty} A_{2j}^{(0)} r_2^j P_j(\cos \theta_2)$$

If p is in the exterior of the dielectric sphere

$$\phi = \phi_1^{(0)} + \phi_{2E}^{(0)}$$

$$= \phi_1^{(0)} + \sum_{j=0}^{\infty} \frac{B_{2j}^{(0)}}{r_2^{j+1}} P_j(\cos\theta_2)$$

 $A_{2j}^{(0)}$  and  $B_{2j}^{(0)}$  are determined by using equations (13) and (14)

$$A_{2j}^{(0)} = \left\{ \frac{\epsilon_E(2j+1)}{(\epsilon_2 + \epsilon_E)j + \epsilon_E} \right\} M_{2j}^{(0)}$$

$$B_{2j}^{(0)} = (R_2)^{2j+1} \left\{ \frac{(\epsilon_E - \epsilon_2)j}{(\epsilon_2 + \epsilon_E)j + \epsilon_E} \right\} M_{2j}^{(0)}$$

4. Re-expand the potential  $\phi_{2E}^{(0)}$  (due to all  $B_{2j}^{(0)}$ ) around  $c_1$  by using equation (18) as

$$\phi_{2E}^{(0)} = \sum_{i=0}^{\infty} M_{1j}^{(1)} r \{ P_j (\cos \theta_1) \}$$

where

$$M_{1j}^{(1)} = \sum_{k=0}^{\infty} (-1)^{j} \frac{1}{d^{j+k+1}} \frac{(k+j)!}{k! j!} B_{2k}^{(0)}$$

5. Use equation (8) to express the potential  $\phi$  in the following form

$$\phi = \phi_1^{(0)} + \phi_{2F}^{(0)} + \phi_1^{(1)}$$

$$\phi_1^{(1)} = \sum_{j=0}^{\infty} \frac{B_{1j}^{(1)}}{r_1^{j+1}} P_j(\cos \theta_1)$$

 $B_{1j}^{(1)}$  is determined by using equation (9)

$$B_{1i}^{(1)} = -M_{1i}^{(1)}R_1^{2j+1}$$

6. Re-expand  $\phi_1^{(1)}$  (due to all  $B_{1i}^{(1)}$ ) around  $c_2$  by using

equation (19) as

$$\phi_1^{(1)} = \sum_{j=0}^{\infty} M_{2j}^{(1)} r_2^j P_j(\cos \theta_2)$$

where

$$M_{2j}^{(1)} = \sum_{k=0}^{\infty} (-1)^k \frac{1}{d^{j+k+1}} \frac{(k+j)!}{k!j!} B_{1k}^{(1)}$$

7. Utilize equations (11) and (12) to express the potential  $\phi$  at  $\mathbf{p}$  in the following forms.

If p is in the interior of the dielectric sphere

$$\phi = \phi_2^{(0)} + \phi_2^{(1)}$$

and if p is in the exterior of the dielectric sphere

$$\phi = \phi_1^{(0)} + \phi_{2F}^{(0)} + \phi_1^{(1)} + \phi_{2F}^{(1)}$$

where

$$\phi_{2I}^{(1)} = \sum_{j=0}^{\infty} A_{2j}^{(1)} r_2^j P_j(\cos \theta_2)$$

$$\phi_{2E}^{(1)} = \sum_{j=0}^{\infty} \frac{B_{2j}^{(1)}}{r_2^{j+1}} P_j(\cos\theta_2)$$

 $A_{2j}^{(1)}$  and  $B_{2j}^{(1)}$  are determined by using equations (13) and (14)

$$A_{2j}^{(1)} = \left\{ \frac{\epsilon_E(2j+1)}{(\epsilon_2 + \epsilon_E)j + \epsilon_E} \right\} M_{2j}^{(1)}$$

$$B_{2j}^{(1)} = (R_2)^{2j+1} \left\{ \frac{(\epsilon_E - \epsilon_2)j}{(\epsilon_2 + \epsilon_E)j + \epsilon_E} \right\} M_{2j}^{(1)}$$

By repeating steps 4 to 7 until the value of  $\phi$  converges, we obtain the final solution of the potential  $\phi$ .

#### REFERENCES

- T.C. Jordan and M. T. Shaw, "Electrorheology", IEEE Trans. EI, Vol. 24, pp. 849-878, 1989.
- [2] Eds: K. O. Havelka and C. F. Filisk, Progress in Electrorheology, Plenum Press, New York and London, 1995.
- [3] S. Takeyama, Denjikigakugenshouriron, Maruzen Publishing Company, pp. 40-48, Japan, 1975 [In Japanese].
- [4] M. H. Davis, "Electrostatic Field and Force on a Dielectric Sphere Near a Conducting Plane - A Note on the Application of Electrostatic Theory to Water Droplets", Amer. J. Phys., Vol. 37, pp. 26-29, 1969.
- [5] R.D. Stoy, "Solution Procedure for the Laplace Equation in Bispherical Coordinates for Two Spheres in a Uniform External Field: Parallel Orientation", J. Appl. Phys., Vol. 65, pp. 2611-2615, 1989.
- [6] R. D. Stoy, "Induced Multipole Strengths for Two Dielectric Spheres in an External Electric Field", J. Appl. Phys., Vol. 69, pp. 2800-2804, 1991.
- [7] M. Washizu and T. B. Jones, "Dielectrophoretic Interaction of Two Spherical Particles Calculated by Equivalent Multipole-moment Method", IEEE Trans. Industry Applications, Vol. 32, pp. 233-242, 1996.
- [8] Y. Nakajima and T. Matsuyama, "Calculation of Pearl Chain Forming Force by Re-expansion Method", J. Inst. Electrostat. Jpn., Vol. 25, No. 4, pp. 215-221, 2001 [In Japanese].
- [9] P. Moon and D. E. Spencer, Field Theory for Engineers, D. Van Nostrand Company Inc., New York, 1961.

- [10] B. Techaumnat, S. Hamada, and T. Takuma, "Electric Field Behavior Near a Contact Point in the Presence of Volume Conductivity", IEEE Trans. DEI, Vol. 8, pp. 930-935, 2001.
- [11] J. Takimoto, "Structure Formation and Dynamics in ER Fluids", J. Inst. Electrostat. Jpn., Vol. 24, No. 6, pp. 298-302, 2000 [In Japanese].
- [12] B. Liu, S. A. Boggs, and M. T. Shaw, "Electrorheological Properties of Anisotropically Filled Elastomers", IEEE Trans. DEI, Vol. 8, pp. 173-181, 2001.
- [13] T. Takuma, "Field Behavior at a Triple Junction in Composite Dielectric Arrangements", IEEE Trans. El, Vol. 26, pp. 500-509, 1991.
- [14] D.K. Cheng, Field and Wave Electromagnetics, Addison-Weslessian 2nd edition, pp. 170-172, 1989.



Boonchaf Techaumnat (M'02) was born in Bangkok. Thailand, on July 24, 1970. He received the B.Eng. and M.Eng. degrees in electrical engineering from Chulalongkorn University, Thailand, in 1990 and 1995, respectively. He received the D.Eng. in electrical engineering from Kyoto University, Japan, in 2001. He has been a Lecturer at the Faculty of Engineering, Chulalongkorn University since 1995. His research interests

include numerical field analysis, electrical insulation, and bioelectromagnetics.



Tadasu Takuma (SM'84-'91) was born in Mie prefecture, Japan, on September 30,1938. He received the B.S., M.S., and Ph.D. degrees in electrical engineering from Tokyo University in 1961, 1963, and 1966, respectively. He joined the Central Research Institute of Electric Power Industry (CRIEPI) in 1967. He served as Visiting Professor of the Graduate School of Engineering Sciences, Kyushu University from

1989 to 1993 and as Professor in the Department of Electrical Engineering, Kyoto University from 1995 to 2002. He is now a research advisor to Komae Research Laboratory, CRIEPI. His principal fields of interest are SF6 gas insulation, gas discharges, environmental problems of overhead transmission lines, numerical field calculation, and new energy problems. Dr. Takuma received the Maxwell Premium from the Institution of Electrical Engineers, Great Britain, in 1974, and twice the book prize from the IEE (the Institute of Electrical Engineers), Japan in 1981 and 1991, and Commendation from the Minister of State for Science and Technology, Japan in 1992.

# Calculation of electric field and dielectrophoretic force on spherical particles in chain

# B. Techaumnatal and B. Eua-arporn

Electrical Engineering Department, Chulalongkorn University, Phyathai, Pathumwan, Bangkok 10330, Thailand

#### T. Takuma

Central Research Institute of Electric Power Industry, 2-11-1 Iwado kita, Komae-shi, Tokyo 201-8511, Japan

(Received 26 June 2003; accepted 7 November 2003)

This article presents an analytical method for calculating electric field and dielectrophoretic force in three-dimensional arrangements of spherical particles. The analytical method is based on the method of images that utilizes the multipole re-expansion and the fundamental solutions for several arrangements of a multipole. It is capable of calculating electric field for various conditions of particles and energization. The method needs much less memory than the already proposed one. The calculation results show that force on a dielectric particle chain in a dielectric fluid depends on the number of particles and the chain direction. However, the maximal attractive and repulsive forces reach their saturation values at about 32 and 12 particles, respectively. When the lower particle of a two-particle chain is in contact with a plate electrode, the dielectrophoretic force on the chain becomes higher on the whole, and it always attracts the chain to the electrode. As a result, the particle chain is stabilized for a wider range of the angle between the chain and the applied field. Neglecting the interaction between the electrodes and particles usually gives adequate accuracy in the force calculation, unless the electrodes are not very close to particles. © 2004 American Institute of Physics. [DOI: 10.1063/1.1637138]

#### I. INTRODUCTION

Dielectrophoretic force is now being utilized in many applications of dielectric materials. For example, the force works so as to align dielectric particles suspended in an electrorheological (ER) fluid in the direction of applied electric field, resulting in the change of the fluid viscosity. The ER fluid has been proposed for a variety of applications, such as the hydraulic valve, clutch, and shock absorber. In such applications, we are usually interested in the force acting on particles, which can be often modeled as dielectric spheres. The force on a particle is closely related to the electric field on its surface, and can be readily calculated once we know the electric field.

For an axisymmetrical arrangement of two dielectric spheres under a uniform electric field, the solutions were reported by Davis<sup>3</sup> and Stoy.<sup>4,5</sup> They utilized a bispherical coordinate system to express the surface of two dielectric spheres. The potential is expressed by an infinite series, of which the coefficients are recursively determined. Although this method has a good rate of convergence, it has the main disadvantage that the number of dielectric spheres is limited to only two.

For a three-dimensional (3D) arrangement of two dielectric spheres, Washizu et al.<sup>6</sup> have presented a method utilizing multipole re-expansion for calculating the electric field and force on the particles. The method is clearly extendable to arrangements of any number of particles. It has been later

applied to an axisymmetrical arrangement consisting of a few tens of particles. However, it is difficult to apply the method for a large number of particles in 3D arrangements. This is because it requires setting up and solving a linear equation system, which becomes much more difficult to solve with an increasing number of particles. Besides, the method has been proposed only for arrangements under a uniform field.

In this article, we present a variation of the analytical method proposed by Washizu et al. Our method is based on the method of images having fundamental solutions for several relevant arrangements, for example, the solutions for a multipole and a spherical dielectric. The main advantages of our approach are: (1) it requires less memory in calculation than the method of Washizu et al. because the solution is obtained by a repetitive procedure instead of forming a linear equation system, (2) particles under consideration may be either conductor or dielectric, and (3) it is applicable for various types of energization, including a uniform field, plate electrodes, and spherical electrodes. We have already proposed a method for axisymmetrical arrangements.8 Here, we extend it to the case of 3D arrangements, and calculate the dielectrophoretic force on particles in a dielectric fluid. We also investigate the effects of various parameters on the force, such as the number of particles, direction of a particle chain, and existence of a planar electrode.

#### II. CALCULATION METHOD

Figure 1 shows an example of arrangements that the analytical method proposed here is applicable for electric field

<sup>\*)</sup>Electronic mail: boonchai.t@chula.ac.th

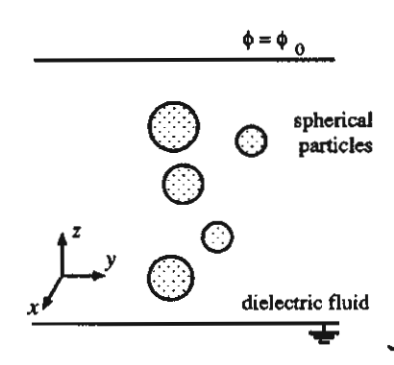


FIG. 1. Dielectric particles suspended in a dielectric fluid.

calculation. In the figure, spherical particles are suspended in a dielectric fluid, which is energized by two parallel-plate electrodes of separation D, having a potential difference  $\phi_0$ . The particles may be dielectrics, floating conductors without net charge, or charged conductors. In general, the method can be applied for arbitrary postitions and radii of particles, although in this article we analyze the electric field and force in arrangements of particle chains. When the parallel-plate electrodes are far from the particles, the field approximates to a uniform field of  $\phi_0/D$ .

The method expresses potential with a set of functions expanded around the origin of spherical coordinates at each particle center. The potentials  $\phi_I$  in the interior and  $\phi_E$  in the exterior of the particle are written as follows:

$$\phi_{i} = \sum_{j=0}^{\infty} \sum_{k=-j}^{j} L_{j,k} r^{j} \bar{P}_{j,[k]}(\cos \theta) e^{ik\psi}, \tag{1}$$

$$\phi_{E} = \sum_{j=0}^{\infty} \sum_{k=-j}^{j} \left\{ \left[ M_{j,k} r^{j} + \frac{B_{j,k}}{r^{j+1}} \right] \tilde{P}_{j,|k|} (\cos \theta) e^{ik\psi} \right\}, \quad (2)$$

where  $L_{j,k}$ ,  $M_{j,k}$ , and  $B_{j,k}$  are the coefficients to be determined,  $(r, \theta, \psi)$  are the spherical coordinates,  $i = \sqrt{-1}$ , and  $P_{i,|k|}$  is the normalized associated Legendre function. The first and second terms on the right-hand side of Eq. (2) can be interpreted as the potentials due to multipoles (including monopoles or point charges) outside and inside the particle being considered, respectively. In our method, we repetitively calculate  $L_{j,k}$ ,  $M_{j,k}$ , and  $B_{j,k}$  for each particle so as to satisfy all the boundary conditions on the particle surface. For a special case in which the particle is a conductor, all the coefficients  $L_{j,k}$ , except  $L_{0,0}$ , are zero. We use the normalized function  $P_{j,|k|}(\cos \theta)$  instead of the associated Legendre function  $P_{j,|k|}(\cos \theta)$  here since  $\bar{P}_{j,|k|}(\cos \theta)$  has better numerical stability at higher values of j and k. The nth-order normalized associated Legendre function  $\overline{P}_{n,|m|}(x)$ ,  $m \in I$ , and  $-n \le m \le n$ , is defined by the equation

$$\bar{P}_{n,|m|}(x) = \sqrt{\frac{(n-|m|)!}{(n+|m|)!}} P_{n,|m|}(x),$$

where  $P_{n,|m|}(x)$  is the associated Legendre function and  $-1 \le x \le 1$ .

The term  $B_{j,k}\bar{P}_{j,|k|}(\cos\theta)e^{ik\psi}/r^{j+1}$  in Eq. (2) is the potential due to the kth component of the jth-order multipole that

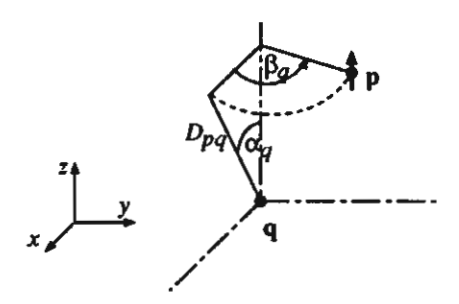


FIG. 2. Re-expansion of the potential due to a multipole at a point p to a point q.  $(D_{pq}, \alpha_q, \beta_q)$  are the spherical coordinates of p when q is taken as the origin.

is located at the particle center. For convenience, we simply regard the term as the potential due to a multipole of orders (j,k) having a strength  $B_{j,k}$ . Note that the definition of strength here is not identical to the conventional definition of multipole moment.

#### A. Multipole re-expansion

Consider a unit multipole of orders (n,m),  $-n \le m$   $\le n$ , located at a point **p** in Fig. 2. The multipole potential is expressed as

$$\phi = \frac{1}{r_p^{n+1}} \bar{P}_{n,|m|}(\cos \theta_p) e^{im\psi_p},\tag{3}$$

where  $(r_p, \theta_p, \psi_p)$  are the spherical coordinates where **p** is taken as the origin. If  $(D_{pq}, \alpha_q, \beta_q)$  are the spherical coordinates of **p** when **q** is taken as the origin (Fig. 2), we can re-expand the potential  $\phi$  to **q** by the equation

$$\phi = \sum_{j=0}^{\infty} \sum_{k=-j}^{j} \left[ A_{n,m,j,k} \tilde{P}_{n+j,|m-k|} (\cos \alpha_q) e^{i(m-k)\beta_q} \right] \times \left( \frac{(-1)^n r_q^j}{D_{pq}^{j+n+1}} \tilde{P}_{j,|k|} (\cos \theta_q) e^{ik\psi_q} \right], \tag{4}$$

for  $r_q \le D_{pq}$ , where  $(r_q, \theta_q, \psi_q)$  are defined in a similar way as  $(r_p, \theta_p, \psi_p)$ , and the coeffcient  $A_{n,m,j,k}$  is determined from the relation

$$A_{n,m,j,k} = i^{|k-m|-|k|-|m|} \sqrt{\frac{(n+m+j-k)!(n-m+j+k)!}{(n+m)!(j-k)!(n-m)!(j+k)!}}$$

Equation (4) is derived from the multipole re-expansion presented by Greengard and Rokhlin.<sup>10</sup> Finally, we rewrite Eq. (4) in the form of more simplified expression as

$$\phi = \sum_{j=0}^{\infty} \sum_{k=-j}^{j} M_{j,k} r_q^j \bar{P}_{j,|k|} (\cos \theta_q) e^{ik\psi_q},$$
 (5)

where the re-expansion moment is given as

$$M_{j,k} = (-1)^n \frac{A_{n,m,j,k}}{D_{pq}^{j+n+1}} \bar{P}_{n+j,|m-k|}(\cos \alpha_q) e^{i(m-k)\beta_q}.$$
 (6)

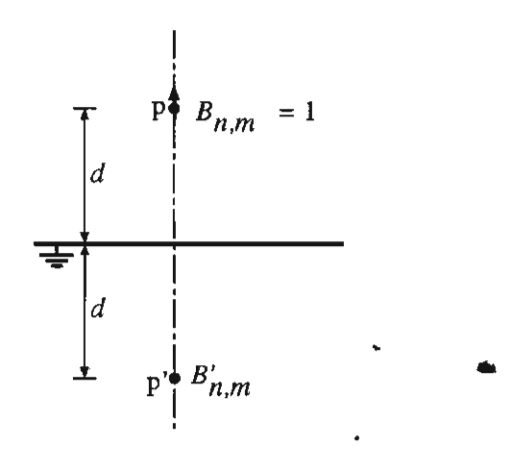


FIG. 3. A unit multipole of orders (n,m) located at p at a distance d above an infinite grounded plane and its image at p'.

#### B. Method of images

The repetitive procedure to calculate electric field is possible if we know the fundamental solutions for configurations composed of a multipole and a particle or an electrode. We present the fundamental solutions for the following arrangements.

#### 1. Multipole and a grounded plane

Consider a unit multipole of orders (n,m) located at a point p that lies at a distance d above an infinite grounded plane, as shown in Fig. 3. Potential due to the multipole is expressed by Eq. (3). We can readily fulfill the zero-potential boundary condition on the plane by placing an image multipole of the same orders at  $\mathbf{p}'$ , which is at the same distance below the plane. The strength  $B'_{n,m}$  of the image multipole is determined by the equation

$$B'_{n,m} = (-1)^{n+m+1}. (7)$$

### 2. Multipole and a grounded spherical conductor

Consider a unit multipole of orders (n,m) located at a point  $\mathbf{p}$  and a grounded spherical conductor, as shown in Fig. 4. The conductor has a radius R and its center is located at a point  $\mathbf{q}$ . Potential due to the multipole is expressed by Eq. (3), and then rewritten in the form of Eq. (5) by re-expanding the potential to  $\mathbf{q}$ . In general, we obtain the fundamental solution for a grounded conductor by placing an infinite number of image multipoles at  $\mathbf{q}$  to satisfy the zero-potential condition on the conductor. The strengths of the image multipoles are related to  $M_{l,k}$  in Eq. (5) by

$$B_{i,k} = -M_{i,k} R^{2j+1}, (8)$$

for j = 0,1,2,... and k = -j, -j + 1,...,j.

It is obvious that the potential is zero on the conductor surface as

$$\phi = \sum_{j=0}^{\infty} \sum_{k=-j}^{j} M_{j,k} R^{j} \bar{P}_{j,|k|} (\cos \theta_{q}) e^{ik\psi_{q}}$$

$$+ \sum_{j=0}^{\infty} \sum_{k=-j}^{j} \frac{B_{j,k}}{R^{j+1}} \bar{P}_{j,|k|} (\cos \theta_{q}) e^{ik\psi_{q}} = 0.$$

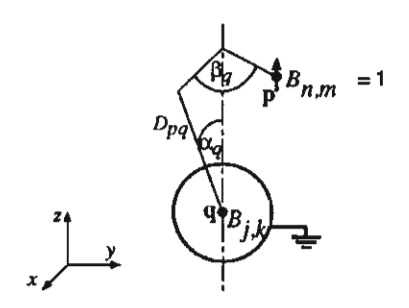


FIG. 4. A unit multipole at p and a spherical conductor.

When the spherical conductor is not grounded, the potential on the conductor is not zero, but total charge on the conductor surface must be equal to a given value (usually zero). We simply fulfill this condition by adjusting the term  $B_{0,0}$  from the just-presented solution since all the other multipoles have no net charge.

### 3. Multipole and a spherical dielectric

Consider again the arrangement in Fig. 4, but now we replace the conductor with a spherical dielectric of radius R. We denote the relative permittivity of the spherical dielectric and its surrounding by  $\epsilon_I$  and  $\epsilon_E$ , respectively. Similarly to the previous section, potential due to the multipole can be rewritten by re-expanding it to  $\mathbf{q}$ , as in Eq. (5). We express the fundamental solutions of the potential  $\phi_I$  in the interior and  $\phi_E$  in the exterior of the spherical dielectric in the forms of Eqs. (1) and (2), respectively, where  $M_{J,k}$  are equal to those in Eq. (5).

To fulfill the boundary conditions of potential and electric field on the dielectric interface, the coefficients  $L_{j,k}$  and  $B_{j,k}$  are related to  $M_{j,k}$  by the following equations:

$$B_{j,k} = \frac{(\epsilon_E - \epsilon_I)j}{(\epsilon_F + \epsilon_I)j + \epsilon_F} R^{2j+1} M_{j,k}, \qquad (9)$$

$$L_{j,k} = \frac{\epsilon_E(2j+1)}{(\epsilon_E + \epsilon_I)j + \epsilon_E} M_{j,k}. \tag{10}$$

### C. Calculation procedure

The procedure to obtain the solutions of  $\phi_I$  and  $\phi_E$  for all particles can be carried out in the following steps.

 Satisfy the initial (potential) boundary condition of each charged conducting particle and each pair of parallelplate conductors as if the other particles or electrodes do not exist.

For a conducting particle possessing a potential  $\phi_p$ , this is accomplished by inserting a point charge

$$q_0 = 4\pi\epsilon_E \epsilon_0 \phi_n R$$

or equivalently, a multipole of orders (0,0), having a strength

$$B_{0.0} = \phi_n R$$
,

where R is the particle radius,  $\epsilon_E$  the relative permittivity of the surrounding medium, and  $\epsilon_0$  is the permittivity of

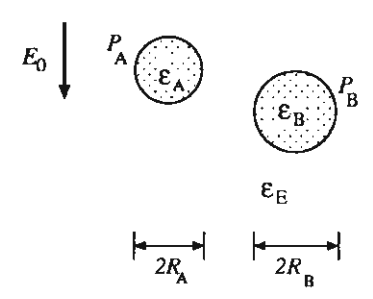


FIG. 5. Two spherical dielectrics under a uniform field  $E_0$ .

free space.

For the parallel-plate conductors in Fig. 1, we simply add a uniform field

$$\mathbf{E}_0 = -(\boldsymbol{\phi}_0/D)\mathbf{a}_z,$$

where  $\mathbf{a}_{z}$  is the unit vector in the field direction.

(2) For each particle and electrode in the arrangement, we consider the potential due to all the external charges, and calculate the interaction between the sources and the particle or electrode.

In this step, we first rewrite the potential as a series of  $M_{j,k}r^{j}\tilde{P}_{j,|k|}(\cos\theta)e^{ik\psi}$ , which is the first term on the right-hand side of Eq. (2). For example, if the particle center is located at a point c, the potential  $\phi_{E0}$  at a point p due to a field  $-E_{0}\mathbf{a}_{z}$  (of parallel-plate electrodes) can be re-expanded to c as

$$\phi_{E_0} = \phi_c + E_0(\mathbf{p} - \mathbf{c}) \cdot \mathbf{a}_z$$
,

where  $\phi_c$  is the potential at c due to  $E_0$ . Now,  $\phi_{E0}$  is rewritten in the form of Eq. (2), in which  $M_{0,0} = \phi_c$  and  $M_{1,0} = E_0$ . For a multipole, we re-expand its potential by using Eq. (5).

After the potential due to all external sources is rewritten, we obtain  $M_{j,k}$  in Eq. (2). We then calculate  $L_{j,k}$  in Eq. (1) and  $B_{j,k}$  in Eq. (2) from  $M_{j,k}$  by the method of images so as to satisfy the boundary conditions on its surface

(3) Repeat the previous step until the solutions of all particles converge.

#### D. Example

Consider an arrangement of two spherical dielectrics,  $P_A$  and  $P_B$  under a uniform electric field  $E_0$  in the -z direction (Fig. 5). The particles of radii  $R_A$  and  $R_B$ , whose centers are at  $\mathbf{c}_A$  and  $\mathbf{c}_B$ , have relative permittivities  $\mathbf{c}_A$  and  $\mathbf{c}_B$ , respectively. The relative permittivity of the surrounding is  $\mathbf{c}_E$ . We assume zero potential at an arbitrary point  $\mathbf{c}_0$ . The potential can be calculated in the following steps, where a subscript A or B of variables denotes their corresponding particle and a superscript (i) indicates the repetition step.

(1) For  $P_A$ , the potential due to  $E_0$  at a point p in its exterior is written as

$$(\phi_A)_E = (\phi_A)_M^{(1)}$$
  
=  $(M_A)_{0,0} \bar{P}_{0,0} (\cos \theta_A) + (M_A)_{1,0} r_A \bar{P}_{1,0} (\cos \theta_A),$ 

where  $(M_A)_{0,0} = \mathbf{E}_0 \cdot (\mathbf{c}_0 - \mathbf{c}_A)$  and  $(M_A)_{1,0} = E_0$ . Similarly, the potential is written for  $P_B$  as

$$(\phi_B)_E = (\phi_B)_M^{(1)}$$

$$= (M_B)_{0.0} \bar{P}_{0.0} (\cos \theta_B) + (M_B)_{1.0} r_B \bar{P}_{1.0} (\cos \theta_B),$$

where  $(M_B)_{0,0}$  and  $(M_B)_{1,0}$  are defined in a similar manner.

(2) Applying the fundamental solution of an arrangement of a multipole and a spherical dielectric for  $P_A$ , we obtain the following expressions:

$$(\phi_A)_E = (\phi_A)_M^{(1)} + (\phi_A)_B^{(1)},$$

$$(\phi_A)_I = (\phi_A)_L^{(1)},$$

$$(\phi_A)_B^{(1)} = \sum_{j=0}^{\infty} \sum_{k=-j}^{j} \frac{(B_A)_{j,k}^{(1)}}{r_A^{j+1}} \tilde{P}_{j,|k|}(\cos\theta_A) e^{ik\psi_A},$$

$$(\phi_A)_L^{(1)} = \sum_{j=0}^{\infty} \sum_{k=-j}^{j} (L_A)_{j,k}^{(1)} r_A^j \bar{P}_{j,|k|} (\cos \theta_A) e^{ik\psi_A},$$

where  $(B_A)_{0,0}^{(1)}$ ,  $(B_A)_{1,0}^{(1)}$ ,  $(L_A)_{0,0}^{(1)}$ , and  $(L_A)_{1,0}^{(1)}$  are calculated from  $(M_A)_{0,0}^{(1)}$  and  $(M_A)_{1,0}^{(1)}$  by using Eqs. (9) and (10), and the other coefficients are zero. Similarly, we obtain the following expressions for  $P_B$ :

$$(\phi_B)_E = (\phi_B)_M^{(1)} + (\phi_B)_B^{(1)},$$

$$(\phi_B)_I = (\phi_B)_L^{(1)},$$

$$(\phi_B)_B^{(1)} = \sum_{j=0}^{\infty} \sum_{k=-j}^{j} \frac{(B_B)_{j,k}^{(1)}}{r_B^{j+1}} \bar{P}_{j,|k|}(\cos\theta_B) e^{ik\psi_B},$$

$$(\phi_B)_L^{(1)} = \sum_{j=0}^{\infty} \sum_{k=-j}^{j} (L_B)_{j,k}^{(1)} r_B^j \bar{P}_{j,|k|} (\cos \theta_B) e^{ik\psi_B}.$$

(3) Using the re-expansion in Eqs. (3)-(6), we re-expand  $(\phi_B)_B^{(1)}$ , the potential due to multipoles inside  $P_B$ , to  $\mathbf{c}_A$ , and obtain  $(\phi_A)_M^{(2)}$ :

$$(\phi_A)_M^{(2)} = (\phi_B)_B^{(1)} = \sum_{j=0}^{\infty} \sum_{k=-j}^{j} (M_A)_{j,k}^{(2)} r_A^j \bar{P}_{j,|k|}(\cos\theta_A) e^{ik\psi_A}.$$

Each coefficient  $(M_A)_{j,k}^{(2)}$  is calculated from all  $(B_B)_{j,k}^{(1)}$  with Eq. (6). Similarly, we re-expand  $(\phi_A)_B^{(1)}$ , the potential due to multipoles inside  $P_A$ , to  $c_B$ , and obtain  $(\phi_B)_A^{(2)}$ :

$$(\phi_B)_M^{(2)} = (\phi_A)_B^{(1)} = \sum_{j=0}^{\infty} \sum_{k=-j}^{j} (M_B)_{j,k}^{(2)} r_B^j \overline{P}_{j,|k|} (\cos \theta_B) e^{ik\psi_B}.$$

(4) Similarly to the second step, we apply the fundamental solution for a mulitpole and a spherical dielectric. For example, for  $P_A$ , we express the potential as follows:

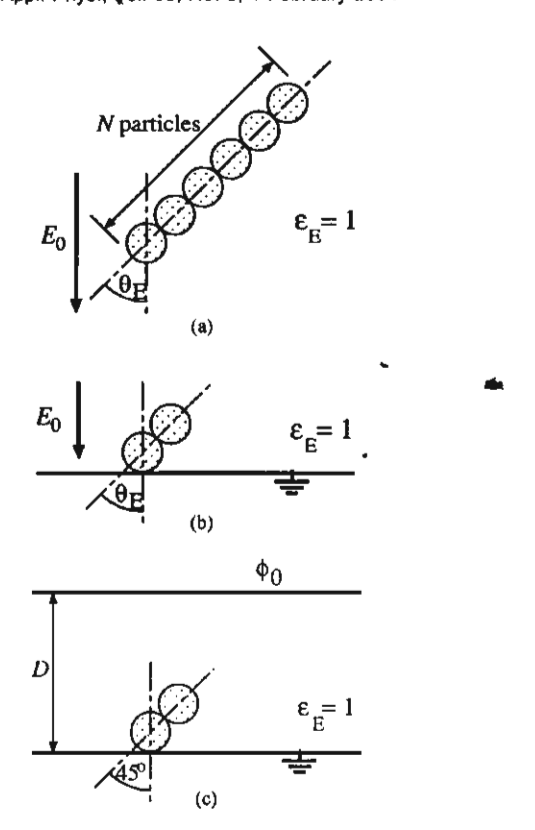


FIG. 6. Dielectric particles in a dielectric fluid ( $\epsilon_E$ : the relative permittivity of the fluid). (a) N-particle chain under a uniform field. (b) Two-particle chain in contact with a plate electrode under a uniform field. (c) Two-particle chain between two parallel-plate electrodes.

$$\begin{split} (\phi_{A})_{E} &= (\phi_{A})_{M}^{(1)} + (\phi_{A})_{B}^{(1)} + (\phi_{A})_{M}^{(2)} + (\phi_{A})_{B}^{(2)}, \\ (\phi_{A})_{I} &= (\phi_{A})_{L}^{(1)} + (\phi_{A})_{L}^{(2)}, \\ (\phi_{A})_{B}^{(2)} &= \sum_{j=0}^{\infty} \sum_{k=-j}^{j} \frac{(B_{A})_{j,k}^{(2)}}{r_{A}^{j+1}} \bar{P}_{j,|k|}(\cos\theta_{A}) e^{ik\psi_{A}}, \\ (\phi_{A})_{L}^{(2)} &= \sum_{i=0}^{\infty} \sum_{k=-j}^{j} (L_{A})_{j,k}^{(2)} r_{A}^{j} \bar{P}_{j,|k|}(\cos\theta_{A}) e^{ik\psi_{A}}, \end{split}$$

where  $(B_A)_{j,k}^{(2)}$  and  $(L_A)_{j,k}^{(2)}$  are calculated from  $(M_A)_{j,k}^{(2)}$  by using Eqs. (9) and (10). The expressions for  $(\phi_B)_E$  and  $(\phi_B)_I$  are in the same forms.

(5) Repeat the two previous steps until the potential value converges.

In the following sections, for arrangements in which a plate electrode exists the fundamental solution for a multipole and grounded plane is applied to satisfy the potential condition on the plane. The fundamental solution for a multipole and grounded spherical conductor is given in Sec. II B for reference. The fundamental solution is not utilized here, but it is necessary for an arrangement having a conductor sphere.

#### E. Force calculation

The dielectrophoretic force on a particle can be calculated from the Maxwell-Helmholtz stress:

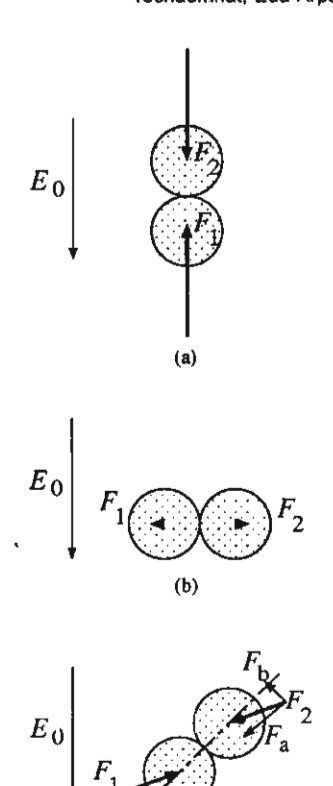


FIG. 7. Dielectrophoretic force on a two-particle chain under a uniform field. (a)  $\theta_E$ =0°. (b)  $\theta_E$ =90°. (c)  $\theta_E$ =45°.

$$\mathbf{f} = \epsilon_F \epsilon_0 \mathbf{E} E_n - \frac{1}{2} \epsilon_F \epsilon_0 E^2 \mathbf{n}, \tag{11}$$

where  $\epsilon_E$  is the relative permittivity of the surrounding medium, E the electric field on particle surface,  $E_n$  the normal component of E, and n the unit normal vector on the surface. Alternatively, it is possible to calculate the force as the sum of that acting on effective multipoles of each particle. However, we calculate the force here by using a straightforward method, integrating the stress over particle surface.

#### **III. CALCULATION ARRANGEMENTS**

We apply the aforementioned method to calculate electric field and force on spherical dielectric particles in arrangements shown in Fig. 6. They consist of dielectric particles in a dielectric fluid energized by two parallel-plate electrodes. As mentioned earlier, dielectrophoretic force in fluids usually attracts particles, resulting in the formation of particle chains. Particle chains in Fig. 6 are assumed bent to form angles  $\theta_E$  against the applied field. Figure 6(a) presents a case in which the electrodes are so far from particles that we can approximate their effect with a uniform field. We have varied the number of particles for  $\theta_E$  ranging from  $0^{\circ}$  to 90°. In Fig. 6(b), a two-particle chain is in contact with a plate electrode, while the other electrode is still away from the particles. We investigate the variation of force with  $\theta_E$ . In Fig. 6(c), in which both plate electrodes are at a finite distance, we study the effect of electrode separation D on the force for  $\theta_E = 45^{\circ}$ . In all the calculations, the particle radius

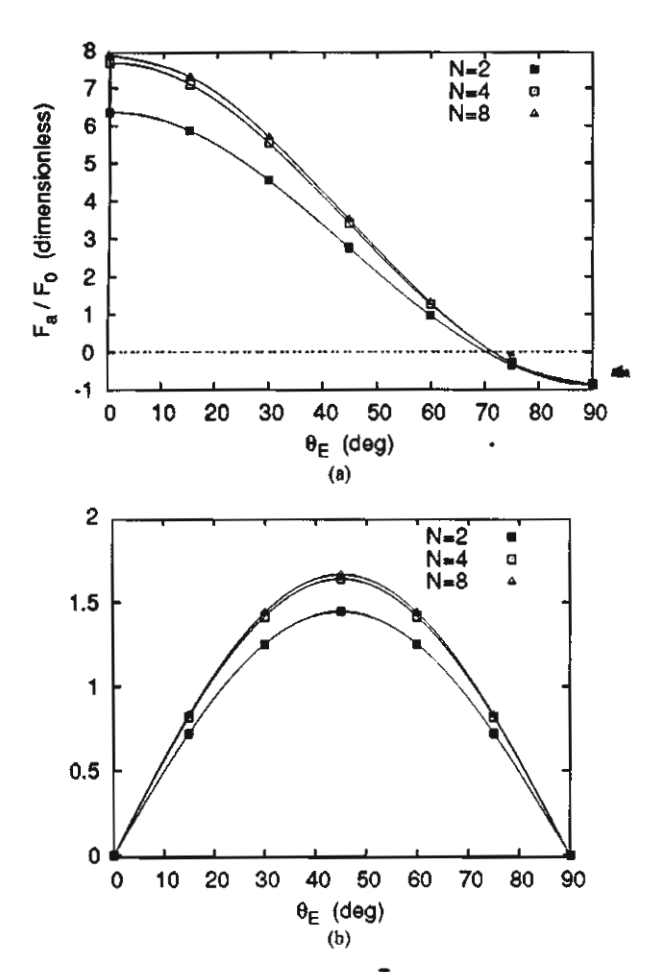


FIG. 8. Forces on the uppermost and lowermost dielectric particles in Fig. 6(a). (a) Component  $F_a$  parallel to the chain direction. (b) Component  $F_b$  perpendicular to the chain direction.

and the applied electric field are set to a unit value, and the relative permittivities of the particles and the fluid are 4 and 1, respectively. The ratio  $\phi_0/D$  in Fig. 6(c) is kept at a unit value so that when no particle exists, the field is the same as that in the other arrangements. In the following section, forces are normalized by  $F_0 = 1/2 \epsilon_0 E_0^2 R^2$  for generality.

### IV. RESULTS AND DISCUSSION

We discuss the effects of the following parameters on the dielectrophoretic force acting on particles in a dielectric fluid.

### A. Angle between applied field and a particle chain

Figure 7 shows the force on a two-particle chain in Fig. 6(a) for  $\theta_E = 0^\circ$ , 45°, and 90°. The vectors  $\mathbf{F}_1$  and  $\mathbf{F}_2$  represent the forces on the lower and upper particles, respectively. The figure illustrates that both magnitude and direction of the forces greatly vary with  $\theta_E$ . For  $\theta_E = 0^\circ$ ,  $\mathbf{F}_1$  and  $\mathbf{F}_2$  are attractive forces parallel to the particle chain, where  $F_1 = F_2 = 6.352F_0$ . For  $\theta_E = 90^\circ$ ,  $\mathbf{F}_1$  and  $\mathbf{F}_2$  are repulsive forces also parallel to the particle chain, but perpendicular to the applied field, where  $F_1 = F_2 = 0.828F_0$ . For  $0^\circ < \theta_E < 90^\circ$ , the forces are not parallel to the particle chain, as

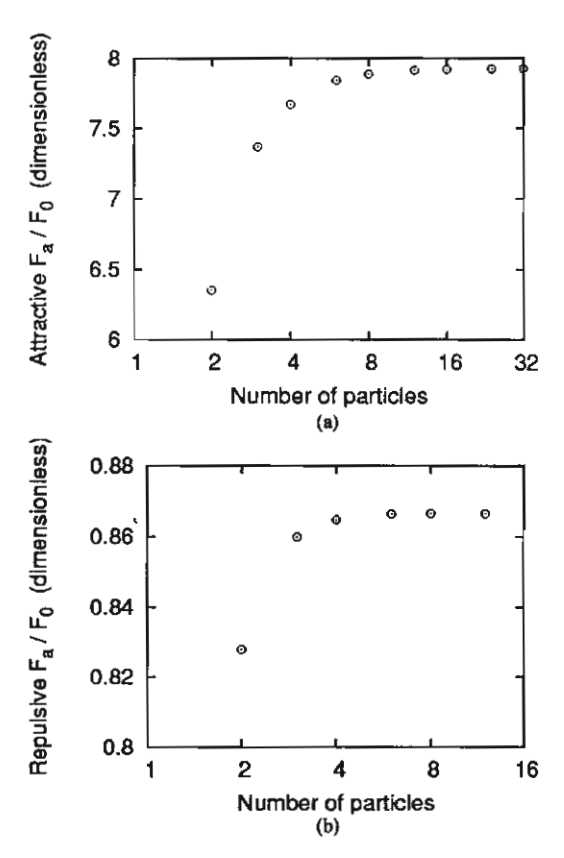


FIG. 9. Variations of the maximal attractive and repulsive forces with the number of particles. in Fig. 6(a). (a) Maximal attractive force ( $\theta_E$ =0°). (b) Maximal repulsive force ( $\theta_E$ =90°).

shown in Fig. 7(c) where  $\theta_E=45^\circ$ . They are composed of two components:  $F_a$  parallel and  $F_b$  normal to the chain direction. Here, we define the signs of  $F_a$  and  $F_b$  such that (1)  $F_a>0$  for an attractive force and  $F_a<0$  for a repulsive one, and (2)  $F_b>0$  for a force that tends to align the chain with the applied field (reducing  $\theta_E$ ). Figure 7 implies that there must be a transition angle that the dielectrophoretic force changes from attractive to repulsive one. The transition angle is about 70° for this two-particle chain. We discuss the transition angle further for chains of more particles in the next session. Our results for a two-particle chain agree well with those of Washizu et al., 6 which were obtained by separating the field  $E_0$  into the components parallel and normal to the chain before calculation.

### B. Number of particles

Figure 8 shows the relation between  $\theta_E$  and  $F_a$  or  $F_b$  on the highest and lowest particles of a particle chain in Fig. 6(a). In the figure,  $F_a$  and  $F_b$  are presented for numbers of particles, N=2, 4, and 8. For each N,  $F_a$  changes from attractive force to repulsive one approximately between 70° and 73° in Fig. 8(a). On the other hand, Fig. 8(b) shows that  $F_b$  never changes its sign; thus, it tends to align the chain with the applied field for all  $\theta_E$ .  $F_a$  is most attractive when  $\theta_E=0^\circ$  and most repulsive when  $\theta_E=90^\circ$ , while the maximal  $F_b$  occurs at  $\theta_E\approx45^\circ$ . The transition angle at which  $F_a$ 

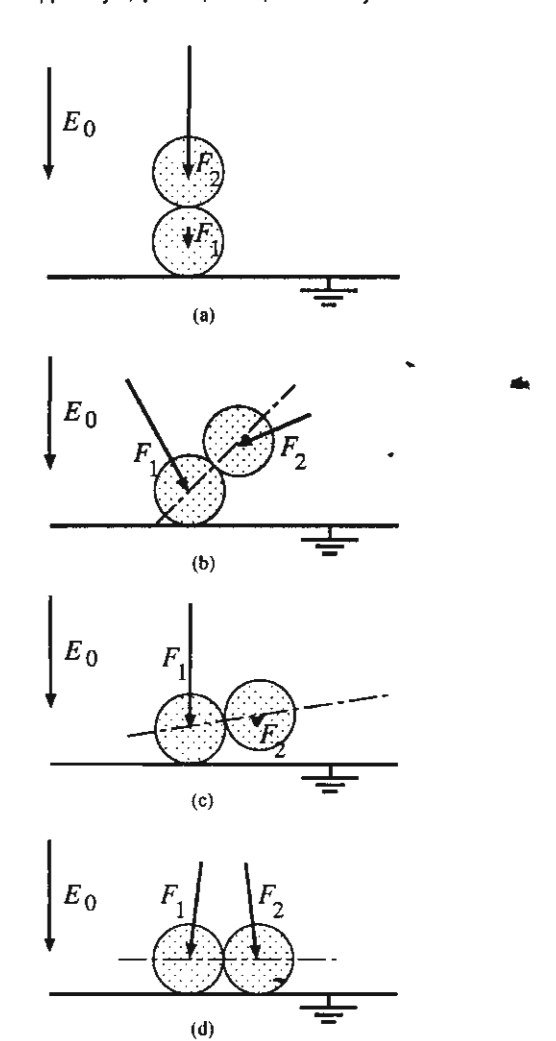


FIG. 10. Dielectrophoretic force on a two-particle chain in contact with a plate electrode. (a)  $\theta_E = 0^{\circ}$ . (b)  $\theta_E = 45^{\circ}$ . (c)  $\theta_E = 80^{\circ}$ . (d)  $\theta_E = 90^{\circ}$ .

changes its sign slightly increases with N. The increase of the transition angle means that a chain is stabilized by dielectrophoretic force for a wider range of the chain direction; however, the effect of N on the transition angle is very small for higher N. The maximal magnitudes of  $F_a$  and  $F_b$  also increase with the number of particles, but this increase becomes saturated with increasing number of particles. Figure 9 shows the variations of the maximal attrative  $F_a$  ( $\theta_E = 0^\circ$ ) and the maximal repulsive  $F_a$  ( $\theta_E = 90^\circ$ ) with the number of particles. Saturation occurs for  $F_a$ , respectively, at  $N \approx 32$  for the maximal attractive force amounting to about  $7.924F_0$  and at  $N \approx 12$  for the maximal repulsive force about  $0.866F_0$ . The saturation of force was also reported by Nakajima et al., but only for the attractive one at  $\theta_E = 0^\circ$ .

#### C. Plate electrodes

Figure 10 shows dielectrophoretic force on the two-particle chain in Fig. 6(b). The angles  $\theta_E$  are 0°, 45°, 80°, and 90° in Figs. 10(a)–10(d), respectively. The variation of  $\mathbf{F}_1$  and  $\mathbf{F}_2$  with  $\theta_E$  significantly differs from that in Fig. 7,

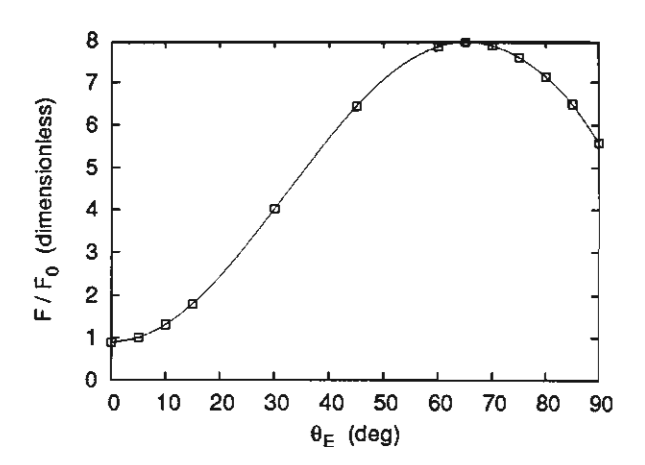


FIG. 11. Force attracting the lower particle to the plate electrode in Fig. 6(b).

where no plate electrode exists. Firstly,  $F_1$  always attracts the lower particle to the plate electrode. Its magnitude is  $0.888F_0$  for  $\theta_E = 0^\circ$ , but becomes substantially higher when  $\theta_E$  increases. Figure 11 presents the component of  $F_1$ , parallel to the field  $E_0$ , attracting the lower particle to the plate

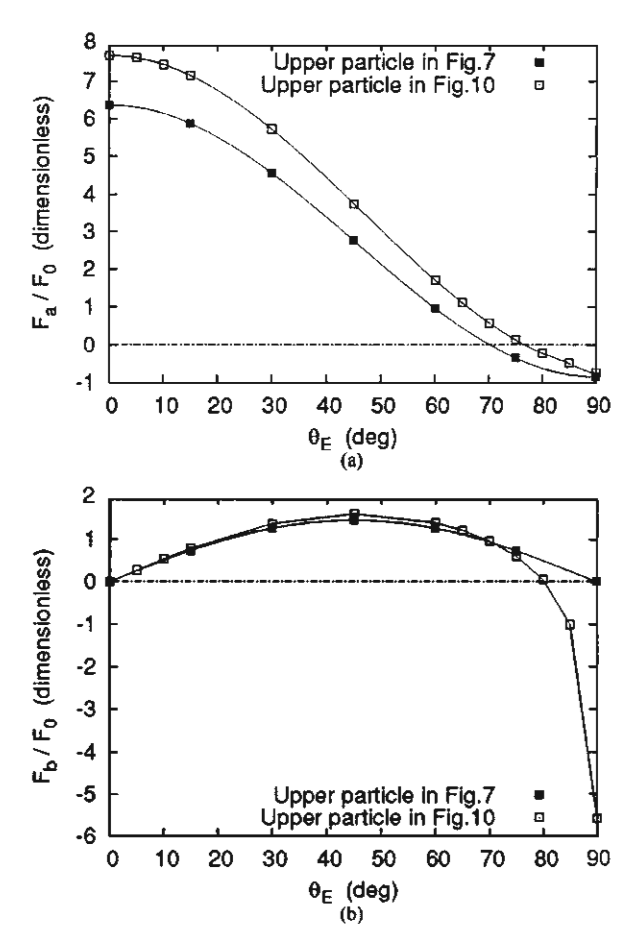


FIG. 12. Comparison of forces on the upper particle in Figs. 7 and 10. (a) Component  $F_a$  parallel to the chain direction. (b) Component  $F_b$  perpendicular to the chain direction.

TABLE 1. Forces on the particles for various D/R in Fig. 6(c), including the case, in Fig. 6(b), of  $D/R = \infty$ .

	Lower particle		Upper particle	
D/R	$F_1/F_0$	ΔF <sub>1</sub> (%)	$F_2/F_0$	ΔF <sub>2</sub> (%)
x.	7.463	0.000	+4.072	0.000
10	7.481	+0.242	+4.082	+0.254
8	7.498	+0.471	+4.093	+0.511
6	7.552	+1.196	+4.127	+1.351
5	7.638	+2.342	+4.181	+2.673
4	7.860	+5.317	+4.311	+5.869

electrode. Secondly, F2 also exhibits the effect of the plate electrode. When  $\theta_E$  is so high that the upper particle becomes very close to the plate electrode, the effect of the electrode is predominant, resulting in an abrupt change of F<sub>2</sub> from Figs. 10(c) to 10(d). Figure 12 compares the components  $F_a$  and  $F_b$  of  $F_2$  in Fig. 10 with those in Fig. 7. The force behavior is similar except the clearly different patterns of  $F_h$  at high  $\theta_E$  in Fig. 12(b). For  $\theta_E$  near 90°, the effect of the plate electrode makes  $F_b$  highly strong downward force for Fig. 10 compared to zero for Fig. 7. For lower  $\theta_E$ , Fig. 12 implies that  $F_2$  in Fig. 10 is similar to that in Fig. 7. However, the attractive force  $F_a$  is stronger for Fig. 10, while the repulsive force is weaker. In conclusion, when a particle chain is in contact with the electrode, the chain is stabilized for a wider range of  $\theta_E$ , and for most values of  $\theta_E$ , the particles are attracted by stronger forces.

For the effect of the upper electrode, Table I presents forces in Fig. 6(c), where  $\theta_E = 45^{\circ}$  for various values of D/R, including the case of Fig. 6(b) as  $D/R = \infty$ . It also shows the difference  $\Delta F$  of the force compared to that for Fig. 6(b). The subscripts 1 and 2 in Table 1 denote the lower and upper particles, respectively. The table shows that the presence of the upper electrode results in a higher dielectrophoretic force. However, for D/R as small as 4, where the separation between the upper particle and the upper electrode is only 0.879R, both  $\Delta F_1$  and  $\Delta F_2$  are still less than 6%. If the upper electrode is extremely close to the upper particle, the force will completely change, as the particle will be attracted to the upper electrode. Such behavior can be inferred from our calculation results for the lower particle in Figs. 6(a) and 6(b).

#### V. CONCLUSIONS

We have presented an analytical method for calculating electric field in 3D arrangements of spherical particles, and applied it to the calculation of the dielectrophoretic force on particles in a dielectric fluid. The method is based on the multipole re-expansion and the method of images, which utilizes fundamental solutions for several arrangements of a multipole. It is capable of calculating electric field for various conditions of particles; for example, dielectric or conductor particles, and energization. Our calculation results show that the force on a particle chain depends greatly on the angle between the applied field and the chain. The maximal attractive and repulsive forces slightly increase with the number of particles in a chain, but they show saturation when the number of particles is high enough. For a twoparticle chain in which the lower particle is in contact with a plate electrode, the force usually attracts the lower particle to the plate electrode and attracts the upper particle to the lower one. The chain is stabilized for a wider range of  $\theta_E$ , and for most values of  $\theta_E$ , the particles are attracted by stronger force. The consideration of the upper electrode in the calculation for  $\theta_E = 45^{\circ}$  gives a stronger force than that obtained for a uniform field or when the upper electrode is neglected. However, the change of force caused by the existence of the upper plate is small, except when the electrode is very close to the particles.

#### **ACKNOWLEDGMENTS**

We want to thank for the support from Thailand Research Fund and Ministry of university affairs, Thailand. We also thank Dr. Shoji Hamada at Kyoto University for his discussions and advice.

- <sup>1</sup>T. Jordan and M. Shaw, IEEE Trans. Electr. Insul. 24, 849 (1989).
- <sup>2</sup> Progress in Electrorheology, edited by K. Havelka and C. Filisk (Plenum, New York, 1995).
- <sup>3</sup>M. Davis, Am. J. Phys. 37, 26 (1969).
- <sup>4</sup>R. Stoy, J. Appl. Phys. 65, 2611 (1989).
- <sup>5</sup>R. Stoy, J. Appl. Phys. 69, 2800 (1991).
- <sup>6</sup>M. Washizu and T. Jones, IEEE Trans. Ind. Appl. 32, 233 (1996).
- <sup>7</sup>Y. Nakajima and T. Matsuyama, J. Inst. Electrostat. Jpn. 25, 215 (2001).
- <sup>8</sup>B. Techaumnat and T. Takuma, IEEE Trans. Dielectr. Electr. Insul. 10, 623 (2003)
- <sup>9</sup>R. Ingarden and A. Jamiołkowski, Classical Electrodynamics (Elsevier, Amsterdam, 1985).
- <sup>10</sup>L. Greengard and V. Rokhlin, Acta Numerica 6, 229 (1997).
- <sup>11</sup>M. Washizu and T. Jones, J. Electrost. 33, 187 (1994).

# Electric field and dielectrophoretic force on particles with a surface film

B. Techaumnata)

Electrical Engineering Department, Chulalongkorn University, Pathumwan, Bangkok 10330, Thailand

#### T. Takuma

Central Research Institute of Electric Power Industry, 2-11-1 Iwado Kita, Komae-shi, Tokyo 201-8511, Japan

(Received 17 May 2004; accepted 4 August 2004)

This article presents the analysis of the electric field and dielectrophoretic force on spherical particles with a surface film. In the analysis, we use the method of images with the fundamental solutions given for the various types of particles composed of a core and a surface film. The concept of the apparent conductivity is introduced to clarify the difference between the particle types. The analysis shows that the response of a particle with a surface film to an external field is unique and generally cannot be obtained by replacing the particle with a homogeneous particle. Using numerical examples, we compare the field and force characteristics between the particles that are of different types but exhibit an identical response to a uniform external field. The electric field and force are found smaller on the conductor-core particle but greater on the dielectric-core particle compared with the particle without any surface film. We have calculated the electric field and force by using the boundary element method in which a surface film is treated as a zero-thickness medium. The propriety of such treatment of a surface film depends not only on the film properties but also on the external field. © 2004 American Institute of Physics. [DOI: 10.1063/1.1801161]

#### I. INTRODUCTION

Dielectric particles commonly exist in applications such as photocopying, printing, and coating. In insulation systems, particles are used as a filler to improve the electrical or mechanical properties of insulators. Another application of dielectric particles that is now widely studied is the electrorheological (ER) fluid, the suspension of the dielectric particles in a host liquid. As the fluid exhibits a fast, reversible change in the apparent viscosity under an electric field, it has been proposed for a variety of applications such as the hydraulic valve, clutch, and shock absorber. Particles utilized in such applications may be homogeneous without any surface layer or may be coated with a surface film. A surface film also occurs as the result of the humidity on particle surface.

For the ER fluid, various types of particles have been proposed to improve the rheological properties of the fluid. In practice, we may classify the particles into three categories: (1) homogeneous particle without any surface element,6 (2) conductor particle with a semiconductive surface film,<sup>7</sup> and (3) insulating particle with a conductive surface film. 10 Since ER response (the change in the apparent viscosity) is a result of the interaction between the particles induced by an applied electric field, several works on ER-response analysis are based on the determination of the electric field and dielectrophoretic force on a two-particle system. Conventionally, particles are modeled as spherical ones in the analysis. The electric field and force have been calculated by the analytical methods, 11-13 numerical methods, 14,15 and an approximation method including the effects of the nonlinear conductivity. The relation between the material properties (permittivity and conductivity of the particles and host liquid) and the fluid behavior has been understood fairly well.

On the other hand, for the ER fluid having particles with a surface film, the fundamental behavior of the particles under electric field has not been fully clear. It is difficult to accurately calculate electric field on the particles with a thin surface film by using numerical field calculation methods. The numerical methods often treat a very thin film as a zerothickness element and introduce the surface conductivity to be a new calculation parameter. 16,17 However, the propriety of such a treatment depends on the film thickness and material properties. Up to now, the electric field and force on a chain of particles with a surface film have been analyzed by using analytical methods in which some approximations on the electric-field distribution are applied. 8,9,18 A typical approximation is that the electric field near the chain axis depends only on the distance from the axis in each medium (core, film, or exterior region). The electric field is then solved to fulfill the conditions of the electric potential and current.

This article presents a fundamental analysis of the electric field and force on particles with a surface film. The objective is to clarify the difference between the homogeneous particle without any surface element and the particle composed of a core and a surface film with respect to the response to an external electric field. We calculate the electric field on particles by the method of multipole images, an analytical method. By the method of images, it is possible to calculate electric field in the arrangements of particles without any approximation on the field distribution. Furthermore, we can make clear how the parameters of the core and the film affect the electric and force behavior. We have already applied the method of multipole images to calculate electric

a)Electronic mail: boonchai.t@chula.ac.th

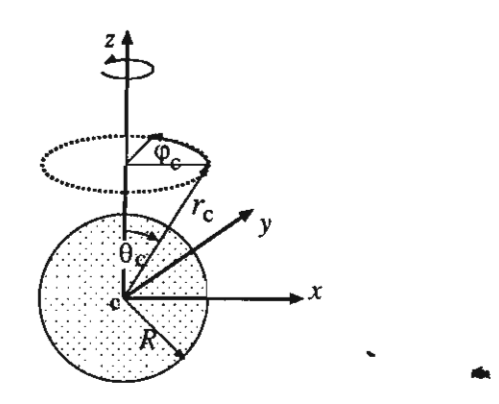


FIG. 1. Spherical particle centered at c.

field and force on systems of homogeneous particles. <sup>12,13</sup> In this article, we present the fundamental solutions for various kinds of particle with a surface film and utilize the fundamental solutions in our analysis.

#### II. SOLUTIONS OF ELECTRIC POTENTIAL

Consider a spherical particle located under an external field  $E_0$ . The particle and the surrounding medium are assumed to possess linear electrical properties independent of the electric field. We can always write the external potential  $\phi_0$  due to the  $E_0$  as a function expanded about the particle center c in the following form:

$$\phi_0 = \sum_{j=0}^{\infty} \sum_{k=-j}^{J} M_{j,k} r_c^j \bar{P}_{j,|k|}(\cos \theta_c) \exp(ik\varphi_c), \qquad (1)$$

where  $M_{j,k}$  is the coefficient of the expansion,  $(r_c, \theta_c, \varphi_c)$  the spherical coordinates having the origin at c (see Fig. 1), and  $\bar{P}_{j,|k'|}$  is the associated Legendre function normalized by  $\sqrt{(j+|k|)!/(j-|k|)!}$ . Note that the external field  $E_0$  is defined here as the field due to all the charges located outside the particle.

The presence of the particle disturbs the potential  $\phi_0$ . In general, if the particle has no surface element, we can separately express the resultant potentials  $\phi_I$  in the interior and  $\phi_E$  in the exterior of the particle as

$$\phi_{j} = \sum_{i=0}^{\infty} \sum_{k=1}^{j} L_{j,k} r_{c}^{j} \bar{P}_{j,|k|}(\cos \theta_{c}) \exp(ik\varphi_{c}), \qquad (2)$$

$$\phi_{\mathcal{E}} = \sum_{j=0}^{\infty} \sum_{k=-j}^{j} \left[ M_{j,k} r_c^j + \frac{B_{j,k}}{r_c^{j+1}} \right] \bar{P}_{j,|k|}(\cos \theta_c) \exp(ik\varphi_c), \quad (3)$$

where  $L_{j,k}$  and  $B_{j,k}$  are the coefficients to be determined so as to satisfy the boundary conditions on the particle surface. If the particle comprises a core and a surface film,  $\phi_I$  in Eq. (2) and  $\phi_E$  in Eq. (3) will represent the potential in the particle core and that in the exterior of the particle, respectively. Additionally, we write the potential,  $\phi_F$ , in the surface film as a function expanded around c as

$$\phi_F = \sum_{i=0}^{\infty} \sum_{k=-i}^{j} \left[ N_{j,k} r_c^j + \frac{O_{j,k}}{r_c^{j+1}} \right] \bar{P}_{j,|k|}(\cos \theta_c) \exp(ik\varphi_c), \quad (4)$$

where  $N_{j,k}$  and  $O_{j,k}$  are the coefficients to be determined. Equations (1)–(4) express the potentials for the general three-dimensional arrangements. For an arrangement where axisymmetry exists, all the nonzero-k terms vanish, and the equations reduce to

$$\phi_0 = \sum_{i=0}^{\infty} M_{j,0} r_c^j \bar{P}_j(\cos \theta_c),$$

$$\phi_I = \sum_{j=0}^{\infty} L_{j,0} r_c^j \overline{P}_j(\cos \theta_c),$$

$$\phi_E = \sum_{j=0}^{\infty} \left[ M_{j,0} r_c^j + \frac{B_{j,0}}{r_c^{j+1}} \right] \bar{P}_j(\cos \theta_c),$$

and

$$\phi_F = \sum_{j=0}^{\infty} \left[ N_{j,0} r_c^j + \frac{O_{j,0}}{r_c^{j+1}} \right] \bar{P}_j(\cos \theta_c).$$

In the following sections, we will describe the solutions of the potentials for the various particles.

### A. Homogeneous particle without a surface film

Let  $\sigma_I$  and  $\sigma_E$  denote the conductivities of the particle and its surrounding medium, respectively. For dc cases (or low-frequency ac cases, where the conductivity is totally predominant over the permittivity), we obtain the following relations between the  $M_{j,k}$  and the other potential coefficients in Eqs. (2) and (3) for  $j \ge 1$ :

$$L_{j,k} = \frac{(2j+1)\sigma_E}{(j+1)\sigma_E + j\sigma_I} M_{j,k},$$
 (5)

$$B_{j,k} = \frac{j(\sigma_E - \sigma_I)}{(j+1)\sigma_E + j\sigma_I} R^{2j+1} M_{j,k}, \tag{6}$$

where R is the particle radius. It can be readily shown that the coefficients given by Eqs. (5) and (6) satisfy the boundary conditions

$$\phi_I = \phi_E,$$
 (7)

$$\sigma_I E_{nI} = \sigma_F E_{nF} \tag{8}$$

on the particle surface  $(r_c=R)$ , where  $E_n$  is the normal component of the electric field and the subscripts I and E denote the corresponding regions. In addition to Eqs. (5) and (6), we always have  $L_{0,0}=M_{0,0}$  and  $B_{0,0}=0$  (except for the charged conductor particles). It is obvious from the equations that if  $\sigma_I=\sigma_E$ , then  $L_{j,k}=M_{j,k}$  and  $B_{j,k}=0$  for all j, i.e., the potential remains equal to  $\phi_0$ .

If the particle is a floating conductor,  $\sigma_I = \infty$ , then  $L_{j,k} = 0$  and  $B_{j,k} = -R^{2j+1}M_{j,k}$  for  $j \ge 1$ . Consequently, the electric

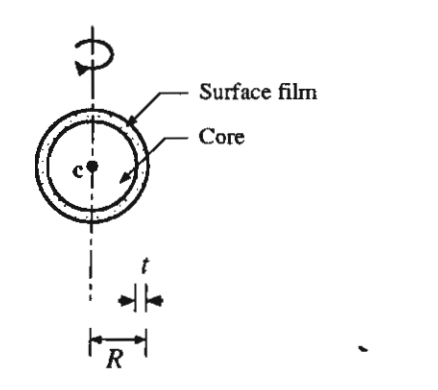


FIG. 2. Particle composed of a core and a surface film.

field inside the conductor is zero. The field  $E_r$  on the conductor surface  $(r_c=R)$  is obtained from the partial derivative of  $\phi_E$  in Eq. (3).

$$E_r = \sum_{j=1}^{\infty} \sum_{k=-j}^{j} -(2j+1)M_{j,k}R^{j-1}\bar{P}_{j,|k|}(\cos \theta_c)\exp(ik\varphi_c)$$

$$= \sum_{j=1}^{\infty} (E_r)_j = \sum_{j=1}^{\infty} \frac{2j+1}{j}(E_{r0})_j,$$
(9)

where  $(E_r)_j$  and  $(E_{r0})_j$  are the (j-1)th-order components of the  $E_r$  and  $-\partial \phi_0/\partial r_c$ , respectively, on the conductor surface. The field-intensification ratio  $(E_r)_j/(E_{r0})_j$  is equal to 3 for j= 1 and constantly decreases with increasing j. The ratio approaches 2 as  $j \to \infty$ . Thus, the field intensification due to a conductor particle is greater for the external field of the lower (j-1)th-order. [The (j-1)th-order field is associated with the jth-order potential.] For the general case of a finite value of  $\sigma_I$  greater than  $\sigma_E$ , the electric field is essentially intensified in the exterior of the particle. The field intensification has a variation with j similar to the case of a conductor particle. However, the degree of the field intensification depends on the ratio of  $\sigma_I/\sigma_E$ . For real fluids, it should be noted that the host-liquid conductivity  $\sigma_E$  substantially increases with the electric field when the field is higher than a critical value. For this case, the increase of  $\sigma_E$  decreases  $\sigma_I/\sigma_E$ , thus mitigating the electric-field intensification in high-field regions. As a result, the maximal field is lower than the value estimated by the constant-conductivity model. Similarly, the real force is also weakened because the force is usually predominated by the high electric field.

# B. Particle composed of a conductor core and a surface film

Figure 2 shows a particle composed of a conductor core and a semiconductive surface film. We shall refer to a particle of this type as a conductor-core particle hereafter. The film thickness and conductivity are denoted by the t and  $\sigma_F$ , respectively. Because the electric field inside the core is theoretically zero, we focus on the potentials  $\phi_F$  in the film and  $\phi_E$  in the exterior of the particle.

The relations between the  $M_{j,k}$  and the other potential coefficients for  $j \ge 1$  are given by the following equations:

$$B_{j,k} = \left\{ \frac{j(1 - \zeta^{2j+1})\sigma_E - [j + (j+1)\zeta^{2j+1}]\sigma_F}{(j+1)(1 - \zeta^{2j+1})\sigma_E + [j + (j+1)\zeta^{2j+1}]\sigma_F} \right\} \times M_{j,k}R^{2j+1}, \tag{10}$$

$$N_{j,k} = \frac{(2j+1)\sigma_E}{(j+1)(1-\zeta^{2j+1})\sigma_E + [j+(j+1)\zeta^{2j+1}]\sigma_F} M_{j,k},$$
(11)

$$O_{j,k} = -R_C^{2j+1} N_{j,k}, (12)$$

where  $R_C$  is the core radius  $(R_C=R-t)$  and  $\zeta$  is the radius ratio defined by  $\zeta=R_C/R$ . Rearranging Eq. (10) into a form similar to Eq. (6), we get

$$B_{j,k} = \frac{j(\sigma_E - \sigma_{Ij})}{(j+1)\sigma_E + j\sigma_{Ij}} R^{2j+1} M_{j,k},$$
(13)

where  $\sigma_{lj}$  is regarded as the apparent conductivity of the particle associated with the (j-1)th-order external field. In other words, if all the components of the external field are of the same (j-1)th order, we can replace the particle by a homogeneous particle having  $\sigma_l = \sigma_{lj}$  and obtain the same electric-field distribution in the exterior of the particle. The apparent conductivity is a function of the film conductivity, the radius ratio, and the order of the external field. For a conductor-core particle,

$$\sigma_{IJ} = \left[ \frac{j + (j+1)\zeta^{2j+1}}{j(1-\zeta^{2j+1})} \right] \sigma_F \quad \text{for } j \ge 1.$$
 (14)

It should be noted here that the similar concept of the apparent material property has already been reported for dielectric mixtures <sup>19,20</sup> and layered spherical particles. <sup>21</sup> However, the concept has been applied only for the case where the external field is uniform or axisymmetrical. In this article, we generalize the apparent conductivity for the three-dimensional cases of an arbitrary external field so as to compare the behavior of the particles having different structures.

# C. Particle composed of a perfect-dielectric core and a surface film

Consider again the particle in Fig. 2, but the particle core is now a perfect dielectric, i.e., it has zero conductivity. We shall refer to a particle of this type as a dielectric-core particle. The potentials  $\phi_E$  and  $\phi_F$  are still expressed by Eqs. (3) and (4), respectively. From the boundary condition of the electric field on the core surface, we can infer that

$$\frac{\partial \phi_F}{\partial r_c} = 0 \quad \text{at } r_c = R_C. \tag{15}$$

The aforementioned condition is also a good approximation for practical particles composed of an insulation core and a film, provided the core conductivity is sufficiently lower than  $\sigma_F$ . To satisfy all the boundary conditions, the potential coefficients of the  $\phi_F$  and  $\phi_E$  conform to the following relations:

$$B_{j,k} = \frac{j}{j+1} \left\{ \frac{[(j+1)+j\zeta^{2j+1}]\sigma_E - (j+1)(1-\zeta^{2j+1})\sigma_F}{[(j+1)+j\zeta^{2j+1}]\sigma_E + j(1-\zeta^{2j+1})\sigma_F} \right\} \times M_{j,k} R^{2j+1}, \tag{16}$$

$$N_{j,k} = \frac{(2j+1)\sigma_E}{[(j+1)+j\zeta^{2j+1}]\sigma_E + j(1-\zeta^{2j+1})\sigma_F} M_{j,k},$$
 (17)

$$O_{j,k} = \frac{j}{j+1} R_C^{2j+1} N_{j,k}. \tag{18}$$

Again, we can rearrange Eq. (16) into the form of Eq. (13), and obtain the following expression for the apparent conductivity of the dielectric-core particle:

$$\sigma_{lj} = \frac{(j+1)(1-\zeta^{2j+1})}{(j+1)+j\zeta^{2j+1}}\sigma_F \quad \text{for } j \ge 1.$$
 (19)

# D. Particle composed of a semiconductive core and a surface film

Although in this article we focus on three particle types described in the previous sections, the concept of  $\sigma_{lj}$  can be applied to general cases where the core is neither a conductor nor a perfect dielectric but has a conductivity  $\sigma_C$ . For the general case, the potentials  $\phi_l$  in the core,  $\phi_F$  in the surface film, and  $\phi_E$  in the exterior of the particle are expressed by Eqs. (2), (4), and (3), respectively.

To fulfill the boundary conditions on the core surface and those on the particle (film) surface, the relations between the expansion coefficients are given by the following equations for  $j \ge 1$ :

$$\frac{B_{j,k}}{M_{j,k}} = R^{2j+1} \left( \frac{j}{j+1} \right) \times \frac{C_1 + C_2 \Gamma_{CF} - C_3 \Gamma_{FE} - C_4 \Gamma_{CE}}{C_1 + C_2 \Gamma_{CF} + C_2 \Gamma_{FE} + [j/(j+1)] C_4 \Gamma_{CE}}, \quad (20)$$

$$\frac{L_{j,k}}{M_{j,k}} = \frac{(2j+1)^2}{j+1} \frac{1}{C_1 + C_2 \Gamma_{CF} + C_3 \Gamma_{FE} + [j/(j+1)]C_4 \Gamma_{CE}}$$
(21)

$$\frac{N_{j,k}}{L_{j,k}} = \frac{(j+1) + j\Gamma_{CF}}{2j+1},\tag{22}$$

$$\frac{O_{j,k}}{L_{j,k}} = \frac{j}{2j+1} (1 - \Gamma_{CF}) R_C^{2j+1},\tag{23}$$

where  $\Gamma_{AB}$  is the conductivity ratio defined by  $\Gamma_{AB} = \sigma_A / \sigma_B$ , and  $C_1$  to  $C_4$  are given by

$$C_1 = (j+1) + j \zeta^{2j+1}$$

$$C_2 = j(1 - \zeta^{2j+1}),$$

$$C_3 = (j+1)(1-\zeta^{2j+1}),$$

$$C_4 = [j + (j+1)\zeta^{2j+1}].$$

Equation (20) can be rewritten in the form of Eq. (13), where the apparent conductivity is given by

$$\sigma_{Ij} = \frac{C_3 + C_4 \Gamma_{CF}}{C_1 + C_2 \Gamma_{CF}} \sigma_F \tag{24}$$

$$= \frac{C_4 + C_3 \Gamma_{FC}}{C_1 + C_3 \Gamma_{CF}} \sigma_C \quad \text{for } j \ge 1.$$
 (25)

It can be readily shown that Eq. (25) reduces to Eq. (14) for  $\sigma_C = \infty$  and to Eq. (19) for  $\sigma_C = 0$ .

Lastly, it should be noted that the fundamental solutions in Secs. II A-II D are given for the dc cases or low-frequency ac cases, where the conductivity is totally predominant over the permittivity. For general cases, we replace  $\sigma$  with the complex conductivity  $\dot{\sigma}$  defined by  $\dot{\sigma} = \sigma + j\omega\varepsilon$ , where  $\varepsilon$  and  $\omega$  are the permittivity and angular frequency of the energization, respectively. Accordingly, in the perfect-dielectric case or in high-frequency ac cases where conductivity can be neglected,  $\sigma$  in the fundamental solutions shall be replaced by  $\varepsilon$ .

#### **III. VARIATION OF THE APPARENT CONDUCTIVITY**

First, it is worth noting that the apparent conductivity  $\sigma_{ij}$  varies with j for both the conductor-core and dielectric-core particles. This, under an external field comprising the components of more than one order, the response of a particle with a surface film to the field is unique and cannot be obtained by replacing the particle with a homogeneous particle. The only exception is the case that the external field consists of components having the same order, e.g., a uniform external field. However, if two or more particles are located not so far from each other, the external field for each particle is the resultant field from the applied electric field and from the charges induced in the other particles. As a consequence, all the field components are not of the same order in a multiparticle configuration.

Next, consider the effect of the film thickness t on  $\sigma_{Ij}$  in Eqs. (14) and (19). For t=R,  $\zeta=0$  and both equations are reduced to

$$\sigma_{Ij} = \sigma_F$$
.

For 0 < t < R (or  $0 < \zeta < 1$ ),  $\sigma_{lj}$  of the conductor-core particle increase, but that of the dielectric-core particle decreases with decreasing t. If no surface film exists  $(t=0 \text{ and } \zeta=1)$ , then

 $\sigma_{Ii} = \infty$  for the conductor core, but

 $\sigma_{Ii} = 0$  for the perfect-dielectric core.

More interesting is the variation of  $\sigma_{ij}$  with j. For j=1, the case of a uniform electric field,

$$\sigma_{Ij} = \frac{1 + 2\zeta^3}{1 - \zeta^3} \sigma_F > \sigma_F$$
 for the conductor core, and (26)